NAVAL POSTGRADUATE SCHOOL

MONTEREY, CALIFORNIA

THESIS

CONTROL STRATEGY: WIND ENERGY POWERED VARIABLE CHILLER WITH THERMAL ICE STORAGE

by

Rex A. Boonyobhas

December 2014

Thesis Advisor: Anthony J. Gannon
Co-Advisor: Anthony G. Pollman

THIS PAGE INTENTIONALLY LEFT BLANK

REPORT DOCUMENTATION PAGE

Form Approved OMB No. 0704–0188

1. AGENCY USE ONLY *(Leave blank)*	2. REPORT DATE	3. REPORT TYPE AND DATES COVERED
	December 2014	Master's Thesis

4. TITLE AND SUBTITLE
CONTROL STRATEGY: WIND ENERGY POWERED VARIABLE CHILLER WITH THERMAL ICE STORAGE

5. FUNDING NUMBERS

6. AUTHOR(S) Rex A. Boonyobhas

7. PERFORMING ORGANIZATION NAME(S) AND ADDRESS(ES)
Naval Postgraduate School
Monterey, CA 93943-5000

8. PERFORMING ORGANIZATION REPORT NUMBER

9. SPONSORING /MONITORING AGENCY NAME(S) AND ADDRESS(ES)
Office of Naval Operations, Technical Monitor: Stacey Curtis, Space and Naval Warfare Systems Command, (ESTEP) Energy Systems Technology Evaluation Program.

10. SPONSORING/MONITORING AGENCY REPORT NUMBER

11. SUPPLEMENTARY NOTES The views expressed in this thesis are those of the author and do not reflect the official policy or position of the Department of Defense or the U.S. Government. IRB Protocol number ____N/A____.

12a. DISTRIBUTION / AVAILABILITY STATEMENT
Approved for public release; distribution is unlimited

12b. DISTRIBUTION CODE

13. ABSTRACT (maximum 200 words)

This study commissioned a variable speed chiller system powered by renewable energy with ice thermal storage. A control strategy was also developed that matched the chiller load to any available renewable power. These solutions will allow the Department of Defense to move away from the traditional, electrical-focused, energy storage methods such as batteries to targeted solutions for large energy uses, specifically cooling. This research required developing a software program to extract data from a micro-grid. In order to effectively use intermittent renewable power, the researcher created a control algorithm for operating the variable speed chiller, and used a monitoring system to match the load to the power production. The data demonstrated that wind energy at the Turbopropulsion Laboratory was intermittent and decreased from summer to fall. The study also created a model to simulate a three-blade vertical-axis wind turbine and compared the results to similar published data. The ANSYS CFX simulation results showed that the NACA0018 blade profile best matched the published result, and was thus selected for additional turbulence modeling. At speeds less than or equal to 10 m/s, the best turbulence for modeling the turbine was the shear stress transport model; at speeds greater than 10 m/s, standard k-epsilon provided the closer correlation.

14. SUBJECT TERMS Thermal Storage, Renewable Energy, Energy Security, Storage Simulation, Facilities Energy

15. NUMBER OF PAGES
85

16. PRICE CODE

17. SECURITY CLASSIFICATION OF REPORT	18. SECURITY CLASSIFICATION OF THIS PAGE	19. SECURITY CLASSIFICATION OF ABSTRACT	20. LIMITATION OF ABSTRACT
Unclassified	Unclassified	Unclassified	UU

NSN 7540–01-280-5500

Standard Form 298 (Rev. 2–89)
Prescribed by ANSI Std. 239–18

THIS PAGE INTENTIONALLY LEFT BLANK

Approved for public release; distribution is unlimited

CONTROL STRATEGY: WIND ENERGY POWERED VARIABLE CHILLER WITH THERMAL ICE STORAGE

Rex A. Boonyobhas
Commander, United States Navy
B.S., University of Maryland, 1994
M.S., University of Mississippi, 1998

Submitted in partial fulfillment of the
requirements for the degree of

MASTER OF SCIENCE IN MECHANICAL ENGINEERING

from the

NAVAL POSTGRADUATE SCHOOL
December 2014

Author: Rex A. Boonyobhas

Approved by: Dr. Anthony J. Gannon
Thesis Advisor

Dr. Anthony G. Pollman
Co-Advisor

Dr. Garth V. Hobson
Chair, Department of Mechanical and Aerospace Engineering

THIS PAGE INTENTIONALLY LEFT BLANK

ABSTRACT

This study commissioned a variable speed chiller system powered by renewable energy with ice thermal storage. A control strategy was also developed that matched the chiller load to any available renewable power. These solutions will allow the Department of Defense to move away from the traditional, electrical-focused, energy storage methods such as batteries to targeted solutions for large energy uses, specifically cooling. This research required developing a software program to extract data from a micro-grid. In order to effectively use intermittent renewable power, the researcher created a control algorithm for operating the variable speed chiller, and used a monitoring system to match the load to the power production. The data demonstrated that wind energy at the Turbopropulsion Laboratory was intermittent and decreased from summer to fall. The study also created a model to simulate a three-blade vertical-axis wind turbine and compared the results to similar published data. The ANSYS CFX simulation results showed that the NACA0018 blade profile best matched the published result, and was thus selected for additional turbulence modeling. At speeds less than or equal to 10 m/s, the best turbulence for modeling the turbine was the shear stress transport model; at speeds greater than 10 m/s, standard k-epsilon provided the closer correlation.

THIS PAGE INTENTIONALLY LEFT BLANK

TABLE OF CONTENTS

I. INTRODUCTION....1
A. RENEWABLE ENERGY....2
B. TARGETED ENERGY STORAGE....3
C. MICRO-GRID SYSTEM....5
D. RESEARCH QUESTION....7
E. LITERATURE REVIEW....7
F. MOTIVATION....10
G. CHALLENGES....11

II. METHODS AND EQUIPMENT....13
A. ENERGY SYSTEM TECHNOLOGY EVALUATION PROGRAM....13
B. EQUIPMENT....14
1. Energy Sources....16
2. Sunny Boys and Island Inverters....18
3. Monitoring and Controlling Systems....19
4. Refrigeration Plant and Thermal Storage....21
C. WIND TURBINE SIMULATIONS....22

III. OBSERVATION AND RESULTS....29
A. EQUIPMENT RESULTS....29
B. WIND TURBINE SIMULATION RESULTS....32

IV. CONCLUSION....37

V. RECOMMENDATIONS....39

APPENDIX A. COMMISSIONING OF THE SUNNY WEB BOX PROCEDURE....41

APPENDIX B. START-UP AND SHUTDOWN PROCEDURE FOR THE MICRO-GRID AT TPL....43
1. Start-up Procedure....43
2. Shutdown Procedure....44

APPENDIX C. ELECTRICAL DRAWINGS OF THE MICRO-GRID PROVIDED BY NEXGEN....45

APPENDIX D. CFD SIMULATION SETTINGS FOR WINDSPIRE ANALYSIS....47

APPENDIX E. MATLAB CODE FOR CREATING THE 3-BLADE ROTOR....53

APPENDIX F. MATLAB CODE FOR MONITORING TURBINE 1 AND 2, AND SUNNY ISLAND STATUS....59

LIST OF REFERENCES....63

INITIAL DISTRIBUTION LIST....67

THIS PAGE INTENTIONALLY LEFT BLANK

LIST OF FIGURES

Figure 1. Gravimetric energy density versus volumetric energy density, from [14]. 4
Figure 2. Regional number of micro-grid based on Navigant Research from fourth quarter 2012. 6
Figure 3. Urban Green Energy (UGE) VisionAIR5 Vertical Axis Wind Turbines on the TPL.....8
Figure 4. A Comparison of Renewable Energy Utilization. 11
Figure 5. Schematic overview of the Micro-Grid System.....14
Figure 6. Micro-grid physical setup at the Turbo Propulsion Laboratory.....15
Figure 7. Integrated system at Turbopropulsion Laboratory, building 216. 15
Figure 8. Start-up cycle controlling strategy for the VFD compressor pump. 17
Figure 9. Layout of the 3 Sunny Islands Inverters. 19
Figure 10. Information flow from micro-grid status to voltage output signal. 19
Figure 11. Sunny Webbox and Asus personal computer monitoring system. 20
Figure 12. National Instrument Analog Input and Output with Chassis. 21
Figure 13. Refrigeration plant for thermal storage. 22
Figure 14. Various blade profiles used for wind turbine simulations. 23
Figure 15. Rotor model created in Solidworks with NACA0018 blade profile. 24
Figure 16. Setup model of the rotor and the stator for simulation. 25
Figure 17. Result of meshing by ANSYS with edge sizing at interface between rotor and stator section.....26
Figure 18. Weekly Alternating Current Production by the UGE Visionaire5 vertical axis wind turbines at the Turbopropulsion Laboratory. Data collected during the months of August through October 2014. 30
Figure 19. Hours of alternating current production during the three months monitoring period at the Turbopropulsion Laboratory. 31
Figure 20. Power versus Wind speed for various NACA blade profiles. 32
Figure 21. C_p versus wind speeds for various NACA blade profiles. 33
Figure 22. Power versus wind speed for NACA0018 profile with a comparison of SST and K-epsilon turbulence model. 34
Figure 23. C_p versus wind speed for NACA0018 profile comparison of SST and k-epsilon turbulence model. 35

THIS PAGE INTENTIONALLY LEFT BLANK

LIST OF TABLES

Table 1. Purchase price of various storage devices per kW-hr, after [14]. 5
Table 2. Simulation conditions for NACA blade profiles. 27
Table 3. NACA0018 simulation condition used for turbulence modeling comparison. 27
Table 4. Power production statistics during the monitor period of August to October 2014. 29

THIS PAGE INTENTIONALLY LEFT BLANK

LIST OF ACRONYMS AND ABBREVIATIONS

AC	Alternating Current
Ah	Amp-hours
AEMR	Annual Energy Management Report
CFD	Computational Fluid Dynamics
COTS	Commercial off the Shelf
C_p	Power Coefficient
DAQ	Data Acquisition
DC	Direct Current
DER	Distributed Energy Resources
DOD	United States Department of Defense
DOE	United States Department of Energy
ESTEP	Energy System Technology Evaluation Program
FNMOC	Fleet Numerical Meteorology and Oceanography Center
FY	Fiscal Year
GFID	Ground Fault Interrupt Detected
gpm	Gallons per Minute
HAWT	Horizontal Axis Wind Turbine
HOMER	Hybrid Optimization of Multiple Energy Resources
Hz	Hertz
ITACS	Information Technology and Communications Services
kW	Kilowatt
kWh	Kilowatt-hour
MCFC	Molten Carbonate Fuel Cells
MRY	Monterey Region Airport
m/s	Meters per Seconds
MW	Megawatt
NACA	National Advisory Committee for Aeronautics
NAVFAC	Naval Facilities
NEDO	New Energy and Industrial Technology Development Organization
NFESC	Naval Facilities Engineering Command

NI	National Instruments
NPS	Naval Postgraduate School
NREL	National Renewable Energy Laboratory
NWTC	National Wind Technology Center
ONR	Office of Naval Research
PSI	Pounds per Square Inch
PV	Photovoltaic
ρ_{air}	Air Density
SI	Sunny Island
SPAWAR	Space and Naval Warfare Systems Command
SST	Shear Stress Transport
STBY	Stand-by
SWBA	Sunny Web Box Assistant
TPL	Turbopropulsion Laboratory
TSR	Tip Speed Ratio
UCSD	University of California, San Diego
UGE	Urban Green Energy
VAC	Volts Alternating Current
VAWT	Vertical Axis Wind Turbine
VDC	Volts Direct Current
VFD	Variable Frequency Drive
VRLA	Valve-regulated Lead Acid
WBI	Wind Box Interface
WT	Wind Turbine

ACKNOWLEDGMENTS

I would like to thank both my advisor and co-advisor, Dr. Anthony J. Gannon and Dr. Anthony G. Pollman, respectively, for many long hours of discussion and guidance through the thesis process. I would also like to extend my gratitude to Noel Yucuis at the Graduate Writing Center for the many hours of thesis reviews, revisions, and discussions. Her patience and professional writing technique proved to be invaluable to the completion of this thesis. I am pretty sure I owe Noel at least one box of pens for all the edits to my thesis.

I would especially like to thank my wife, Onvipa Pongsriwat, for all the emotional support and guidance throughout my career and life in general. She is also a fantastic chef and a great motivator.

THIS PAGE INTENTIONALLY LEFT BLANK

I. INTRODUCTION

According to the Environmental and Energy Study Institute, the largest consumer of U.S. energy is the Department of Defense (DOD) [1]. Energy consumption in the Department of Defense (DOD) is segregated into two categories, operational energy and facility energy [2]. It is the researcher's opinion that the commissioning of micro-grid systems that use technologies such as photovoltaic cells and wind turbines to harness renewable energy will eventually lead to future government installations shifting away from fossil fuel use.

Modern U.S. military operations require enormous amounts of computing power to support troops on the ground [3]. This computing power is used to monitor weapons systems, analyze weather patterns, communicate with allied forces, and even assess the status of power grids. Over the past couple of decades, the United States has been in conflicts with countries in the Middle East. During the summers, the temperature in that part of the world can reach 136 degrees Fahrenheit [4]. Refrigeration plants are the normal means by which the electrical components are cooled. A typical refrigeration plant requires fossil fuel to power its generator. Fossil fuels pose a logistical problem that requires transportation through hostile combat environments, thus endangering U.S. military personnel [3]. Renewable energy sources have the potential to make the United States and its allies less reliant on both fossil fuels and long, vulnerable logistics trains.

Facilities energy is the second category of DOD energy consumption. In fiscal year (FY) 2013, DOD facilities consisted of almost 300,000 buildings, consuming four billion dollars in energy costs [2]. Based on the DOD's *Annual Energy Management Report* (AEMR), facility energy enhancements has been made by "increasing the supply of renewable" and "reducing facility energy demand" [2]. Over the past 10 years, the DOD has increased renewable energy consumption by five percent and reduced facility energy by over 17 percent [2]. These improvements are in line with the three pillars of the DOD's Facility Energy Program:

- Energy efficiency and demand reduction,

- Expansion of energy production (renewable and on-site generation), and
- Leverage advanced technology. [2]

There have been improvements to facility energy, but there is still work to be done since The DOD and its components (Army, Navy, Marine Corps, and Air Force) did not meet the goals for FY13. The goals were to increase usage of renewable energy to 7.5 percent and reduce in facility energy intensity by 24 percent [2].

This thesis focuses on a paradigm shift from the typical electrical company's production of energy that matches load demand to a system that matches loads to available power. U.S. dependency on fossil fuels, and by extension, its dependency on foreign fuel sources, compromises energy security and weakens the economy [5]. As a part of wider research at the Turbopropulsion Laboratory, this thesis focuses on commissioning a micro-grid and controlling the load to closely match the renewable energy supplied to a variable frequency drive compressor of the refrigeration plant. The overall intent is to find novel ways to reduce energy costs and, in doing so, improve the energy security of the DOD facilities.

A. RENEWABLE ENERGY

The United States Department of Energy (DOE) defines renewable energy as being obtained from regenerative sources that cannot be depleted. For the sake of this thesis, renewable energies include solar, wind, geothermal, biomass, and thermal gradients in ocean water [6]. Renewable energy provides benefits to both the military and private sectors. Moreover, renewable energy may enable U.S. independence from foreign oil imports. On the battlefield, less fossil fuel usage equates with a decreased risk to military personnel due to a reduction of military convoy requirements. For U.S. Department of Defense (DOD) facilities and the private sector, renewable energy can be used as an alternative at times when the commercial grid is unavailable, during periods of elevated tariffs, during outages or when surge demand requires it. Furthermore, the majority of renewable energy sources are clean, meaning that apart from the initial manufacturing of the equipment, there are no pollutants emitted into the atmosphere

when being used to power electrical equipment. Zero-emission sources provide the added benefit of reducing the greenhouse gases that cause climate change [7]. Although renewable energy provides a potentially unlimited source of energy, there are several disadvantages. Foremost, because renewable energy is intermittent, it may not be available when the demand for energy is high. Second, renewable energy can be unpredictable, for example, wind energy can only be predicted accurately to approximately 72 hours into the future [8]. Third, renewables often lack sufficient energy density for the application in question.

Of the renewables, solar and wind energy collection technologies are the most mature. Photovoltaic (PV) cells or solar thermal cells are two of the more common ways to harness solar energy. While photovoltaic cells convert photon energy to electrical voltage, the solar thermal cells use heat energy from the sun to run a generator to produce electricity [9]. To harness wind energy, myriad wind turbines are currently available in the commercial market. A wind turbine operates in reverse of an electrical fan. As the wind blows, the rotor of the turbine is driven by the blade to generate shaft power to drive an electrical generator or other device. Two common types of wind turbines are the horizontal axis wind turbine (HAWT) and the vertical axis wind turbine (VAWT). For this thesis, two vertical axis wind turbines will power a refrigeration plant with a variable speed compressor pump to produce ice.

B. TARGETED ENERGY STORAGE

Although technology for collecting renewable energy has vastly improved over the past several decades, one of the biggest remaining challenges is storage of the collected energy. In order to reduce intermittency, renewable energy systems often require a stable storage sub-system to ensure that power is available when needed. Batteries, superconductors, regenerative fuel cells, compressed air, fly wheels, and pumped water storage are various forms of energy storage targeted to electrical energy storage [10]. Nearly 50 percent of energy consumption in the U.S. is applied toward heating or cooling and thus targeted thermal solutions are worth investigating [11]. Additionally, water can be used to store thermal energy in the form of hot or cold

temperature. In heat storage, electrical resistance energy is stored in bricks that are heated to over 1,400 degrees Fahrenheit [12]. In cold storage, water can be converted to ice with a chiller. In order to change the phase of water from solid to liquid, additional heat is required known as latent heat of fusion. This phase change absorbs a large amount of energy with a value of 334 kJ/kg for water [13]. The control of cold storage is examined in this thesis based on the need for data center cooling and the supply of air conditioning for building facilities during the summer in regions of hot temperature.

In comparing water versus batteries for energy storage, there are several advantages to water. First, water is less expensive than batteries. Second, the cycle life of water is over 10,000, limited by the container life not by water itself, as opposed to the charge cycle in batteries, which has a limit of only several thousand cycles [14]. In her thesis, Lindsay Olsen [14] conducted a cost analysis of the thermal storage versus batteries. Ice storage is comparable to lead acid batteries for energy density. The benefits of using ice storage are lower cost per kilowatt-hours and nearly unlimited cycle of usage.

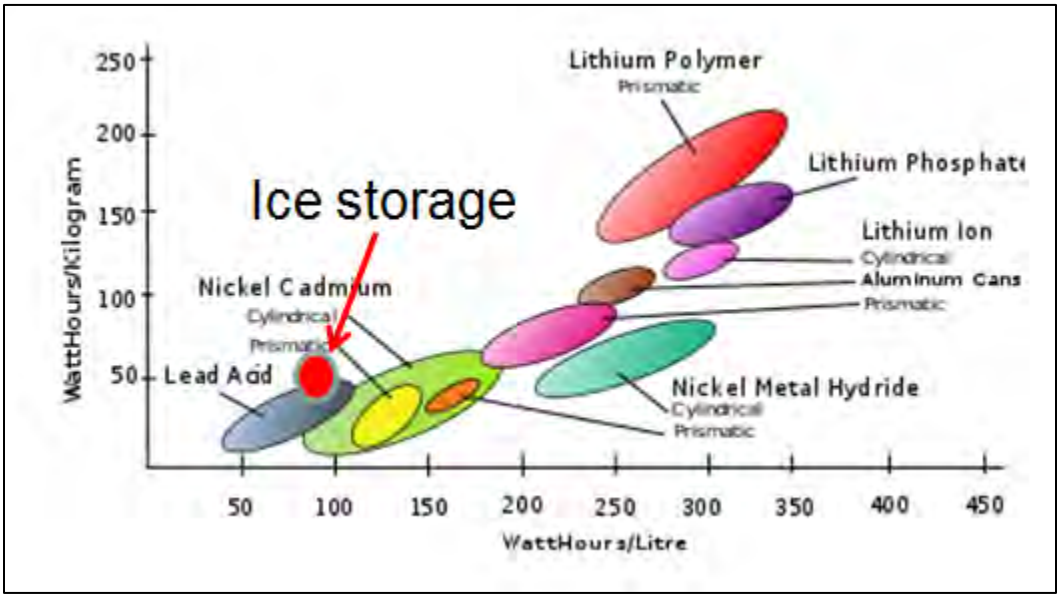

Figure 1. Gravimetric energy density versus volumetric energy density, from [14].

The result of a cost analysis of the thermal storage versus batteries is shown in Table 1.

Thermal ice storage	Alkaline-cell battery	Lead-acid battery	Lithium-ion battery
$37/kW-hr	$140/kW-hr	$150/kW-hr	$400/kW-hr

Table 1. Purchase price of various storage devices per kW-hr, after [14].

Olsen found that thermal storage costs approximately 3.5 times less than the lowest battery per kilowatt-hour (kW-hr) with a life for ice storage of greater than 10,000 cycles. Even though the energy density of ice storage is comparable to a lead acid battery, the benefits of lower cost and large cycling capability make ice a strong candidate for energy storage.

C. MICRO-GRID SYSTEM

Most electrical appliances in the United States are optimized for grid operation and usually require a 3-phase 60 Hz sinusoidal power source. A micro-grid system connects various renewable energy sources together to supply a required load. Simply put, the micro-grid system is a commercial power grid but only on a smaller scale. A micro-grid system generally consists of the following main components: distributed energy resources (DERs), an energy storage device, and an electrical load [15]. Distributed energy sources may include arrays of solar PV cells, solar thermal cells, wind turbines, or biogas digestors. Energy storage devices could consist of one or more of the following: a battery bank, a superconductor, or molten carbonate fuel cells. Micro-grid supplies power to electrical loads. These loads can take various forms: resistors that dissipate energy as heat, refrigeration plants that stores thermal energy, or electricity directly supplied to a residential house or commercial building.

Countries around the world are testing and using micro-grids for back-up and independent power systems. In Kythnos Island, Greece, a micro-grid supplies power to 12 houses. This micro-grid consists of a 10 kilowatt (kW) PV, a 53 kilowatt-hour (kWh) battery bank, and a 5-kilowatt diesel generator [16]. The Kythnos Island micro-grid uses the SMA inverters similar to the ones used in this thesis. In Mannheim-Wallstadt, Germany, a micro-grid has supplied power to over 1,200 people since 2006 [16]. In 2007, Denmark, Italy, Portugal, Spain, the United Kingdom, and the Netherlands also performed research and development on micro-grid systems [16]. Japan is leading its region in developing micro-grids. At Hachinohe, Japan, the Aomori Project obtains up to 100 kW of power from PV cells and wind turbines (WTs). The New Energy and Industrial Technology Development Organization (NEDO) demonstrated its first micro grid at the 2005 World Exposition. The Aichi project consisted of two molten carbonate fuel cells (MCFC) of 270 kW and 300 kW, respectively [16]. As of 2012, North America has over 67 percent of the total number of micro-grids around the world, as illustrated in Figure 2 [17].

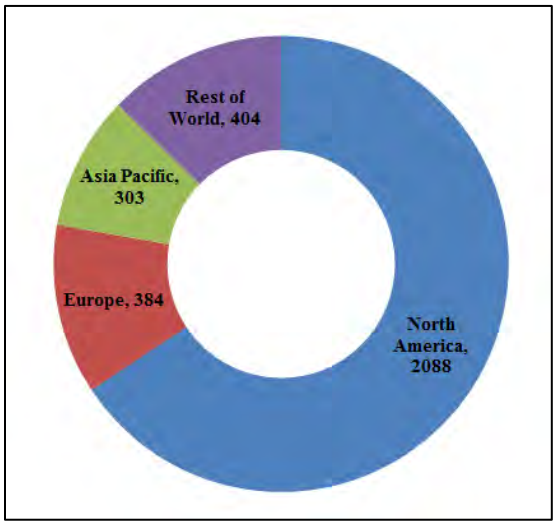

Figure 2. Regional number of micro-grid based on Navigant Research from fourth quarter 2012.

The University of California, San Diego (UCSD) has one of the largest micro-grids in the United States. This micro-grid typically extracts 3 megawatts (MW) of

electricity from the commercial grid, but during times of high load demands, it can supply up to 2 MW of electricity to assist the commercial grid [18]. Solar and wind energy are the sources of renewable energy for the UCSD micro-grid [18].

D. RESEARCH QUESTION

Wind energy is intermittent; hence to be able to provide a reliable source of power, a system must be designed that effectively stores the excess energy that is available when the power demand increases. In light of the conditions at the Naval Postgraduate School's Turbopropulsion Laboratory, how feasible will renewable energy be when used to power a variable speed pump refrigeration plant with a micro-grid? More specifically, how accurately can the load of the refrigeration plant match the incoming renewable energy?

E. LITERATURE REVIEW

According to a 2012 Department of Energy report, U.S. commercial and residential requirements for cooling and refrigeration accounted for 14 percent and 13 percent of energy consumption, respectively [11]. This combined 27 percent of energy usage formed the motivation for this thesis.

In 2010, Brandon Newell conducted a detailed study of energy integration and planning system using Hybrid Optimization of Multiple Energy Resources (HOMER), a computer modeling program, to assess the conditions in the Monterey Bay area [19]. Newell's research focused on the modeling of a grid-tied-PV system at the Naval Postgraduate School (NPS). His research compared HOMER's results to an experiment he ran for a month. His measurements and HOMER's results correlated closely, varying only 17 percent after taking into account temperature effects and "true" solar irradiance [19]. However, when he attempted to compare the results of a system composed of two different types of PV cells and one small wind turbine to Homer's simulation, the results showed a variation of approximately 3,700 percent [19]. Furthermore, Newell's research used a horizontal-axis wind turbine that was unable to compensate for turbulence in the wind to produce electricity. The horizontal-axis wind turbine is generally more efficient than a vertical-axis wind turbine [20]. In order for the HAWT to operate efficiently, the

blades must be positioned perpendicular to the wind. In a confined space, such as on top of a building or a residential home, a HAWT is not practical due to larger blade size and wind direction requirements. In contrast to a HAWT, a VAWT is able to capture wind from all horizontal directions. Additionally, a VAWT operates at a much lower sound power level than a HAWT. Specifically, a HAWT can be as loud as 98 decibels, equivalent to noise due to crossing traffic on a busy highway, versus the VAWT operating at 38 decibels, equivalent to a whispered conversation and often less than the ambient noise of a regular operating refrigerator [21]. The VAWTs at the TPL, shown in Figure 3, operates very quietly even at winds of greater than 20 mph. Even when the turbines are rotating at 130 revolutions per minute they would go unnoticed unless a passerby happens to glance up at the turbines.

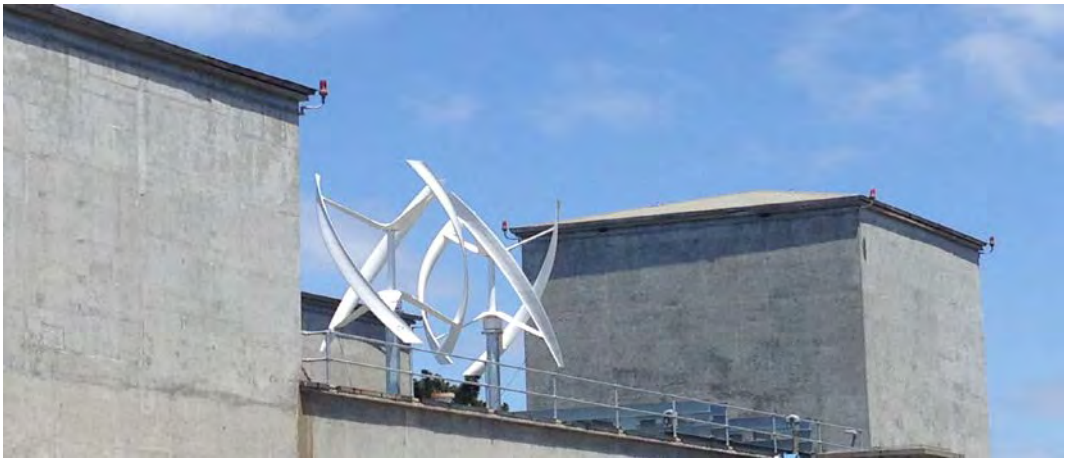

Figure 3. Urban Green Energy (UGE) VisionAIR5 Vertical Axis Wind Turbines on the TPL.

In 1989, Holly Davis from the University of Colorado illustrated the limitation of using a conventional icemaker that used a single speed compressor pump to operate a refrigeration plant [22]. Her work demonstrated that wind turbines can effectively collect energy to produce ice. However, one of the major problems identified in her work was that a large starting current was required for making ice [22]. The large starting current was due to the high start-up torque for a reciprocating compressor of the refrigeration plant.

Davis provided the motivation for two follow-on research projects by NPS students Katharin Taylor and Lindsay Olsen in 2013. Taylor's research focused on the feasibility of installing two vertical axis wind turbines (VAWTs) on top of a building at the Turbopropulsion Laboratory (TPL) [23]. She analyzed the wind flow in the vicinity of the TPL for optimal VAWT placement. Her study also showed that close spacing between two or more VAWTs would amplify the wind effects [23]. Taylor's model compared three separation distances: 0.01 m, 0.1 m and 0.4 m. The power coefficient is a measurement of how efficiently a wind turbine converts wind to mechanical energy, shown in Equation 1 [23]:

$$C_p = \frac{P}{\frac{1}{2}\rho_{air} A V^3}\ , \tag{1}$$

where P is the power, ρ_{air} is the air density, A is the frontal area of the wind turbine, and V is the wind speed. Taylor found a 13 percent increase in the power coefficient and average torque for the distance of 0.1 m versus 0.4 m.

Olsen conducted an in-depth analysis of wind data in the Monterey Bay area over a period of 14 years, from 1998 to 2012 [14]. She modeled the total energy captured by a VAWT during an average year. Additionally, she used ANSYS Workbench, a simulation program, to analyze anticipated ice growth as part of the design for the refrigeration plant at the TPL. Furthermore, she designed and integrated several commercially available components for a refrigeration plant system.

In 2013, Julio Pascual et al. implemented and controlled a micro-grid system that supplies a residential house in Spain [24]. In this work, an electric water heater was used as opposed to a refrigeration plant to store thermal energy (hot thermal energy as opposed to cold thermal energy). The work illustrates a reduction of peak loading during maximum power consumption from the commercial grid. Additionally, this system had batteries and super capacitors to store excess energy produced by a wind turbine and photovoltaic cells [24].

Unlike Davis' work, this research will use a variable frequency drive (VFD) to operate the icemaker. The VFD starts at a lower speed; takes advantage of more modern power electronics and has a 'soft start' capability that slowly accelerates the motor using variable frequencies that allows a small starting current to be used [25]. Both Taylor's and Olsen's theses assisted in creating the initial building blocks for constructing this research. Unlike Pascual, et al. work, this thesis will use a three-phase 208-volt alternating current system and power a refrigeration plant to store ice as thermal energy. The commissioning of a micro-grid with VFD pump and chillers that are powered by two VAWTs is the main thrust of this specific research. Additionally, this research monitors the incoming power from the wind turbine and then matches the loads to the available power using a digital to analog output controller.

In order to control load based on the amount of incoming wind energy, a controller must be used to provide signals to the VFD pump and chillers.

F. MOTIVATION

The first challenge for commissioning a new system is to monitor the inputs of renewable energy and use these input to form the basis for controlling the load of the micro-grid. The second challenge is determining a method to control the system. For this particular system, the input is wind energy collected by two VAWTs. The output is thermal energy storage by conversion of water into ice for subsequent reserve cooling applications.

The chillers will be used as the load for this system with glycol as the working fluid. This more direct conversion of wind energy to ice production should, in theory, prove more effective than conversion of wind energy to battery storage, which later requires conversion back to electricity. This is because there is corresponding energy loss with each electrical to chemical conversion and a far shorter life of the batteries. Figure 4 provides a visual comparison of this concept. The capital investment and operational cost are more important in a renewable energy system than a traditional fossil fuel energy system because the energy source is free. Thus, efficiency is not as important in this renewable powered micro-grid system.

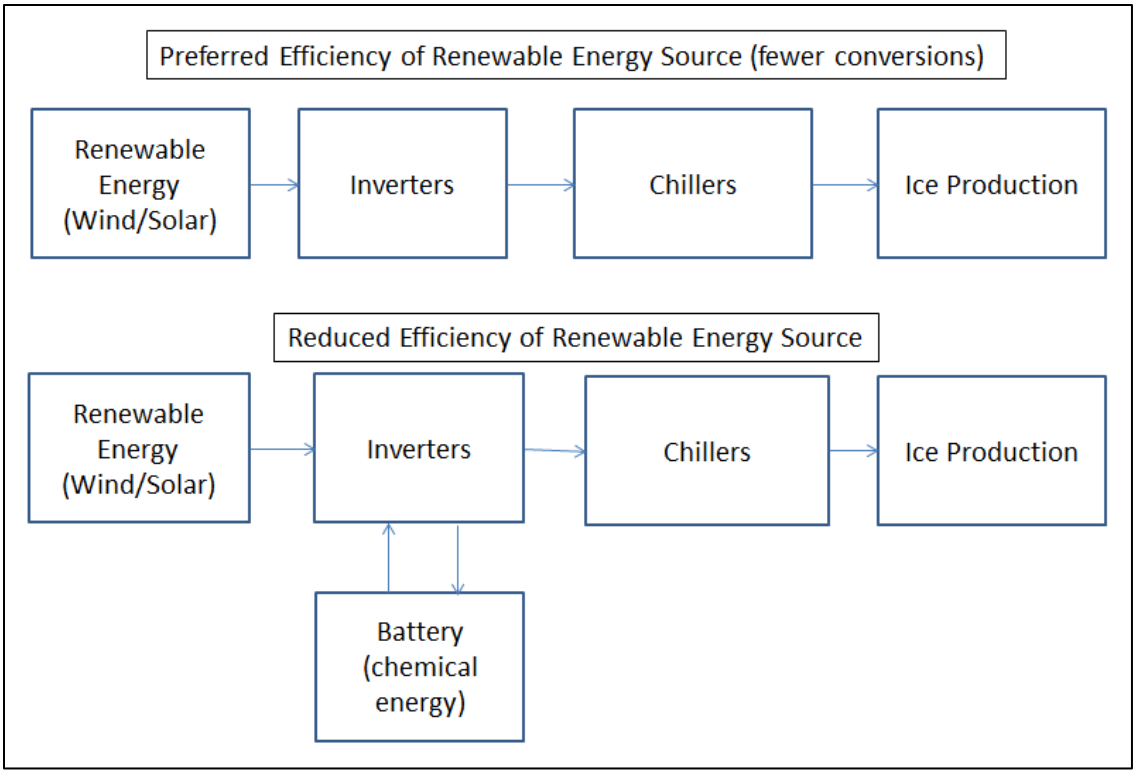

Figure 4. A Comparison of Renewable Energy Utilization.

In reality, some form of electrical storage is needed as you can never follow the wind or renewable load perfectly. The storage can take the form of either small batteries or super capacitors due to use of thermal storage being the main energy reservoir for this targeted system.

G. CHALLENGES

The integration of several commercially available components for the set-up of the micro-grid poses several unique challenges. These challenges were:

- Entering all parameters precisely ensures that the components produce accurate results.
- Obtaining certain specially-designed components prolonged the installation time of equipment.
- Enabling proper monitoring of the system status is vital to controlling loads that use real-time power production from renewable energy sources.

For this research, the wind provided renewable energy. In order to introduce electricity from the wind to the micro-grid, several inverters were installed. The inverters had to be programmed prior to producing electricity. Wind power is essential to programming the Sunny Boy inverters. During the installation of the micro-grid and wind turbines, the period of wind availability was not significant enough to program both wind turbines. Hence, only one wind turbine was programmed during the initial installation. Moreover, private contractors were required to program the inverters.

In order to minimize the initial power surge during the start-up of the refrigeration plant, a specially designed variable-speed chiller unit was manufactured. The refrigeration plant served as the load for this micro-grid. However, this specially designed pump delayed the installation time by nearly four months. Furthermore, the compressor pump must be capable of accepting a zero-to-ten VDC input signal for controlling its speed based on the incoming power of the wind. Due to this delay, a detailed power production analysis by the wind turbines was difficult to assess.

Effective ice production required a real-time data and monitoring system. The traditional method for communicating between electrical equipment is the Modbus architecture, designed in 1979 [26]. Communication between the Sunny Webbox and Master Sunny Island inverter relied on the Modbus architecture. The data power produced was displayed on a webpage created by the Sunny Webbox. It appears that a more efficient method to obtain specific data can be done by extracting the information directly using a Modbus client such as Modbus Poll, Modbus Tool, or MATLAB. However, Modbus communications in this research yielded sporadic results and proved to be unusable for controlling the refrigeration plant. Attempts to contact SMA-America for appropriate coding proved to be unsuccessful.

II. METHODS AND EQUIPMENT

A. ENERGY SYSTEM TECHNOLOGY EVALUATION PROGRAM

The Office of Naval Research (ONR) provides funding and oversight to the Energy System Technology Evaluation Program (ESTEP) [27]. ESTEP was created in 2013 to answer the call of Secretary of the Navy Ray Mabus for increased research into alternative energy sources. Space and Naval Warfare Systems Command (SPAWAR), NPS, and Naval Facilities/Naval Facilities Engineering Service Center (NAVFAC/NFESC) are three main participants in ESTEP [27]. SPAWAR performs program management, provides info/network security expertise, and facilitates technical and business training. NAVFAC/NFESC performs project management, provides facility expertise, and facilitates technical and business training. NPS conducts energy return on investment (ROI) research for energy, provides student project participation, and technical and business education. ESTEP objective is

> To provide the baseline data required for inclusion into energy efficiency systems and equipment procurement specifications. The technology focus will be on innovative pre-commercial and nascent commercial energy technologies obtained from open market sourcing, including companies from within the venture capital and small business communities. [27]

Hence, ESTEP is an excellent architecture in which individuals at NPS can conduct research. The participation of military member leverages fleet experience and enhances utilization of renewable energy in facilities. Furthermore, ONR program officer Sharon Beermann-Curtin explains, "ESTEP is a great opportunity to put alternative energy programs on Navy and Marine Corps bases, and really understand how it's going to work in the field. [28]"

After graduating from NPS, military students can assisting in implementing and promulgating the ESTEP objectives out to the fleet. ESTEP concept should both promote the knowledge of energy usage and improve future implementation of renewable energy systems.

B. EQUIPMENT

In line with ESTEP philosophy, the equipment for this thesis was purchased using commercial-off-the-shelf components whenever possible. The energy sources, the inverters, and the monitoring and control system make up the three main parts of the micro-grid. A schematic of the TPL micro-grid system is shown in Figure 5. The micro-grid can easily incorporate additional equipment due to its modular design.

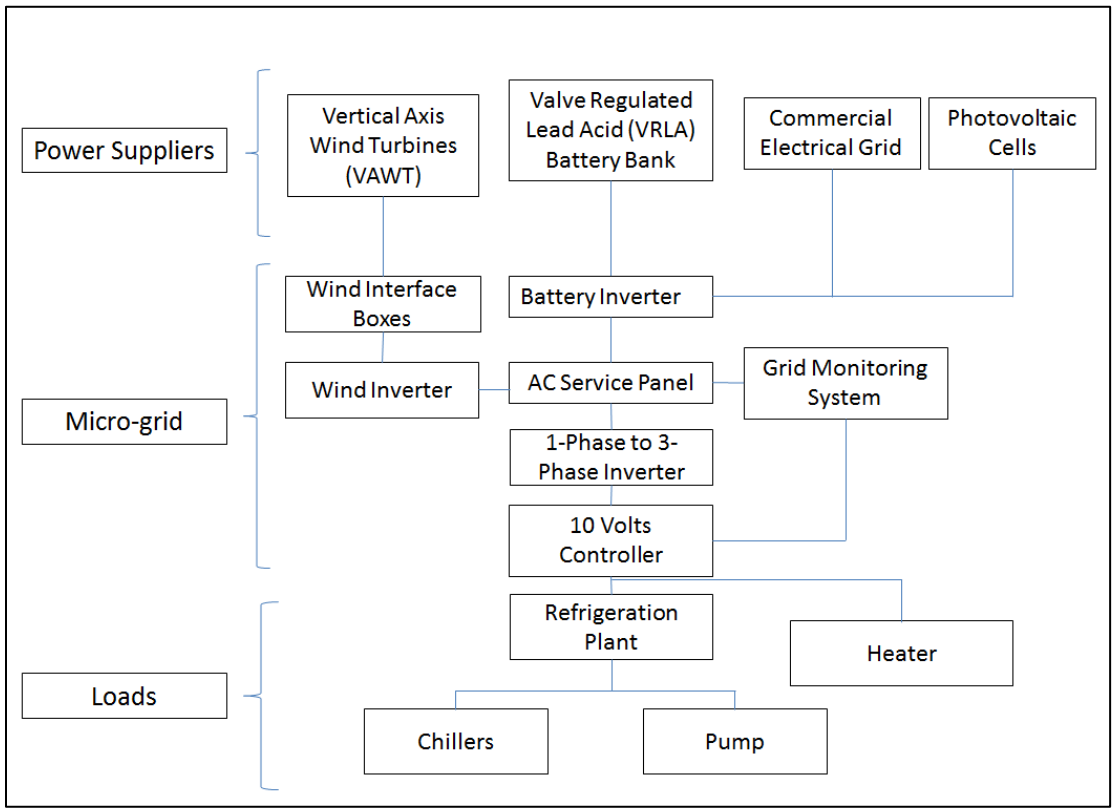

Figure 5. Schematic overview of the Micro-Grid System.

The micro-grid actual setup inside building 216 of the TPL is depicted in Figure 6.

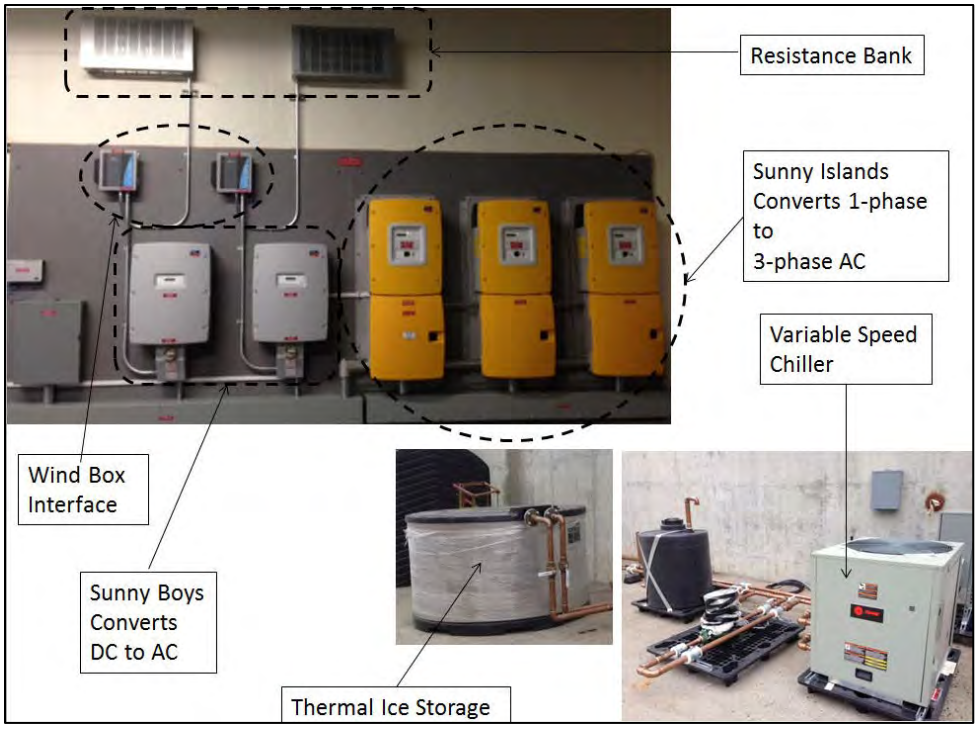

Figure 6. Micro-grid physical setup at the Turbo Propulsion Laboratory.

An integrated Solidworks model of system created by LT Themba Hinke is shown in Figure 7 [12]. This model assisted in the physical placement of the equipment of the refrigeration plant, solar thermal cells, and photovoltaic cells.

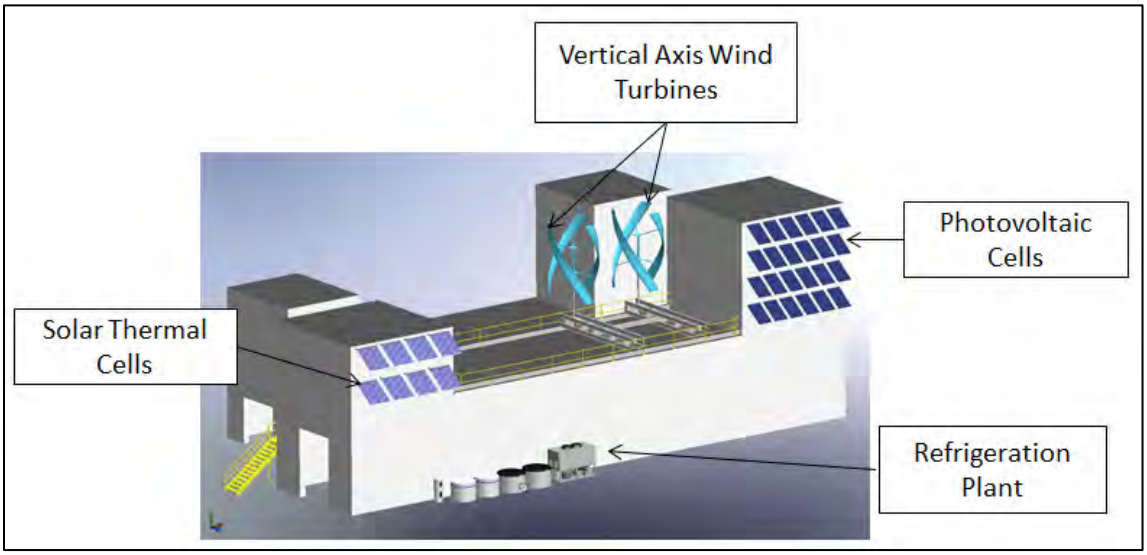

Figure 7. Integrated system at Turbopropulsion Laboratory, building 216.

The solar thermal and photovoltaic cells will be incorporated into the micro-grid for future research.

1. Energy Sources

As shown in Figure 3, the energy is supplied to the micro-grid via two vertical axis wind turbines (VAWTs), the commercial electrical grid, or valve-regulated lead acid (VRLA) batteries. The commercial grid will be used to verify whether the refrigeration plant operates properly prior to switching to the renewable energy source.

The second energy source, the Deka Unigy II VLRA battery is composed of 24 2-volts cells in three cell modules configured into stacked four modules high. The battery is capable of supplying a nominal capacity of 91–200 amp-hours (Ah) at 77 degrees Fahrenheit. The battery serves as storage for surge capacity during the start-up cycle of the refrigeration plant. Five to ten minutes are required to start-up the refrigeration plant; a continuous power ensures that proper lubrication. Figure 8 illustrates the strategy of start-up of the variable frequency drive motor on the compression pump and refrigeration plant. For start-up controls, the MATLAB code will be used to monitor the power that comes into the micro-grid from the wind turbines, solar panels, or main grid. Based on available power, the VFD will slowly ramp up to 25 percent power. Due to the intermittency of wind, four consecutive readings of electricity being produced by the wind turbine is required prior to the VFD compressor pump initiating the start-up cycle for the refrigeration plant. If the renewable energy source is the only power available for operating the refrigeration plant at start-up, the VRLA battery serves as the back-up source in case renewable energy is lost.

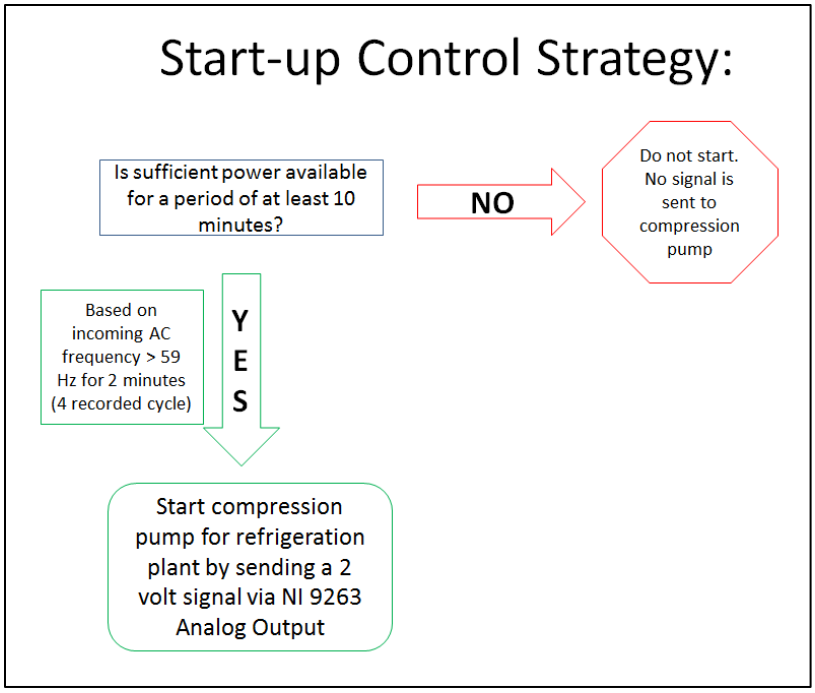

Figure 8. Start-up cycle controlling strategy for the VFD compressor pump.

Once the refrigeration plant has been operational for the 10-minute lubrication period, the control algorithm will shift over to continuous power operation. This control algorithm will examine the incoming renewable power at a rate of one reading every 30 seconds, or 0.033 Hz, and then vary the speed of the chiller to match this available power. Although it is not possible to perfectly match the load to the incoming power, by tracking the incoming power closely, the battery storage capacity can be greatly reduced. When the wind no longer provides sufficient power then a zero VDC signal will be sent to the chiller control unit, thus shutting down the refrigeration plant.

The wind turbines are VisionAIR5 vertical-axis wind turbine manufactured by Urban Green Energy (UGE). The two wind turbines are 5.2 m tall and 3.2 m wide and each capable of producing 3.2 kW electrical power. The cut-in wind speed is 3.5 m/s or 8 miles per hour (mph) with the maximum power wind speed occurring at 14 m/s, 31 mph. The cutout speed is 20 m/s, 44 mph. The VAWTs provide “Wild Alternating Current (AC)” that is rectified by the two Power One PVI-7200 wind box interfaces (WBI). Wild AC has varying frequency and voltage based on dynamic wind conditions. The WBI

converts the "Wild AC" into direct current (DC) that enters the inverters. Diversion loading control, overvoltage protection, and wind speed feedback are the other purposes of the WBI. When the rectified DC voltage exceeds 530 volts DC (VDC), the WBI diverts the electrical flow to the resistance bank to dissipate the energy as heat. The diverted electrical flow discontinues when the voltage drops to less than 430 VDC. If the rectified DC voltage exceeds 600 VDC, then the overvoltage protection in the WBI activates the embedded crowbar, thus lowering the impedance to less than one Ohm [29].

2. Sunny Boys and Island Inverters

The micro-grid consists of two sets of inverters manufactured by SMA Solar Technology. These inverters are called the Sunny Boy and Sunny Island inverters. Each of the Sunny Boy inverters converts the VDC from the WBI into a one-phase 208 Volts AC (VAC). Additionally, the Sunny Boy also contains a system for detecting ground fault errors. The Sunny Boy turns off when a ground fault of greater than 1 ampere is detected. The Sunny Boy displays the fault on an LED screen as a GFID or ground fault interrupt detected. Next, each of the one-phase 208-VAC from the two Sunny Boys feed the master Sunny Island inverter. The master Sunny Island is the left most Sunny Island has shown in Figure 9. The master Sunny Island monitors the other two Sunny Islands by the RJ45 cable. The master Sunny Island connects to the "slave one" Sunny Island, which in turn connects to the "slave two" Sunny Island. The Sunny Island inverters serves several purposes: first, they monitor the state of charge of the VRLA battery and optimally maintains the battery charge; second, the Sunny Islands provide the third phase of a 208 VAC 60 hertz (Hz) three-phase; third, it transmits the micro-grid condition to the Sunny Webbox to be displayed as a web page on a computer. Figure 6 shows the Sunny Islands, Sunny Boys, Resistance Bank, Wind box interfaces that are installed at the TPL.

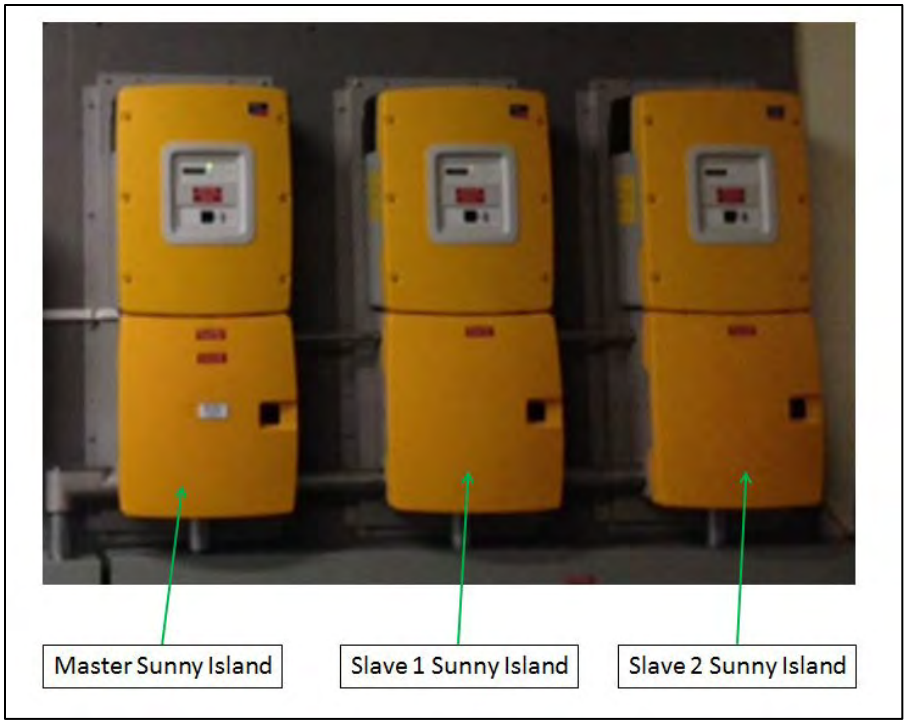

Figure 9. Layout of the 3 Sunny Islands Inverters.

3. Monitoring and Controlling Systems

The MATLAB software is used to record and assess the condition of the incoming power. If the start-up condition is met for the refrigeration plant, a signal is sent to the National Instrument (NI) chassis to produce an output voltage. The NI chassis model is Compact Data Acquisition (cDAQ) 9184. Figure 10 illustrates this flow of information.

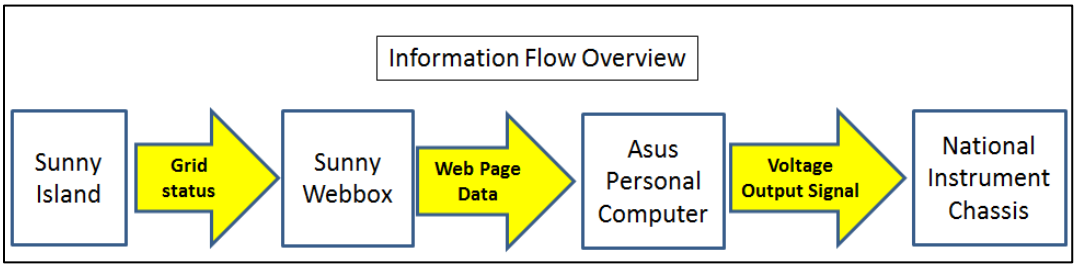

Figure 10. Information flow from micro-grid status to voltage output signal.

Figure 11 shows the Sunny Webbox and an Asus personal computer use for monitoring and displaying the micro-grid status as a webpage. The MATLAB program extracts data from the Sunny Webbox on an interval of every 30 seconds.

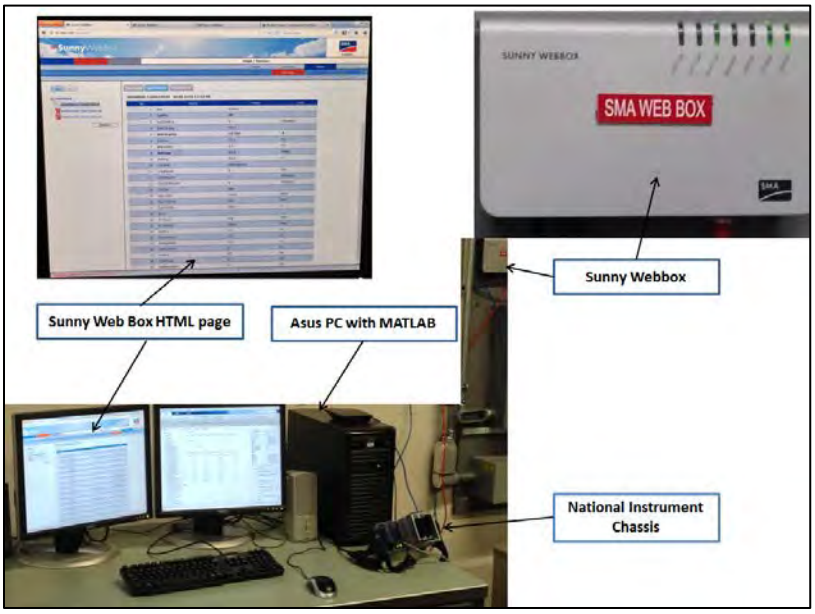

Figure 11. Sunny Webbox and Asus personal computer monitoring system.

The chassis transmits the voltage output signal to the analog output module, NI 9263, 4-Channel, 100 kS/s, 16-Bit, ±10 V. A zero to ten-volt output signal controls the amount of power that supplies the variable speed compressor for the chiller. Figure 12 illustrates the analog output module for controlling the variable frequency drive (VFD) compressor pump. The NI 9201 analog input module is also attached to the chassis for future research to monitor the power consumption of the refrigeration plant.

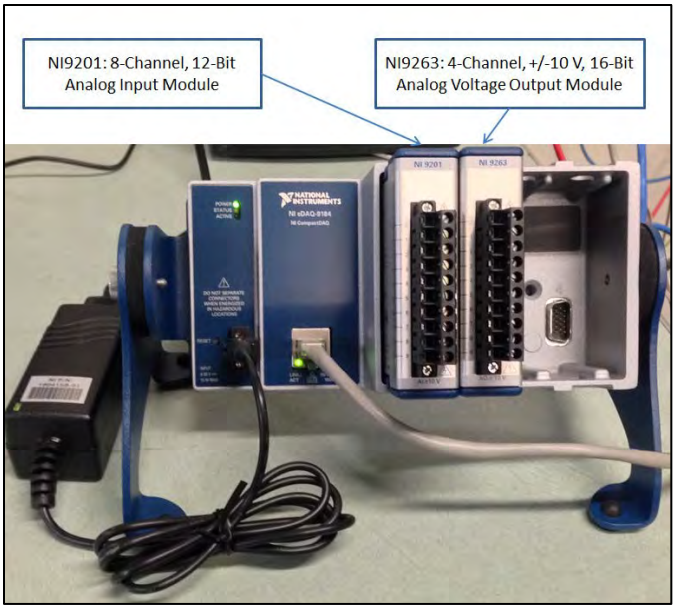

Figure 12. National Instrument Analog Input and Output with Chassis.

4. Refrigeration Plant and Thermal Storage

The refrigeration plant consists of four main components. The first component is the Trane custom outdoor chiller. The chiller provides 7.5 tons of cooling capacity to produce the ice in the thermal storage tank. A 0–10V DC controlled VFD compressor pump is located inside the chiller unit. The second component is the VFD chilled water circulation pump. The water pump is designed for outdoor use with a capacity of 24 gallons per minute (gpm). The Trane/CALMAC thermal storage tank for ice is the third component of the refrigeration plant. The thermal storage tank has a capacity of 410 gallons and has an ice inventory meter attached. The refrigerant storage tank makes up the forth component. It holds propylene glycol refrigerant which is used to freeze water. Propylene glycol, as opposed to ethylene glycol, was selected based on its lower toxicity and more environmentally friendly makeup, it is considered to be food-grade chemical. Figure 13 provides an illustration of the refrigeration plant layout.

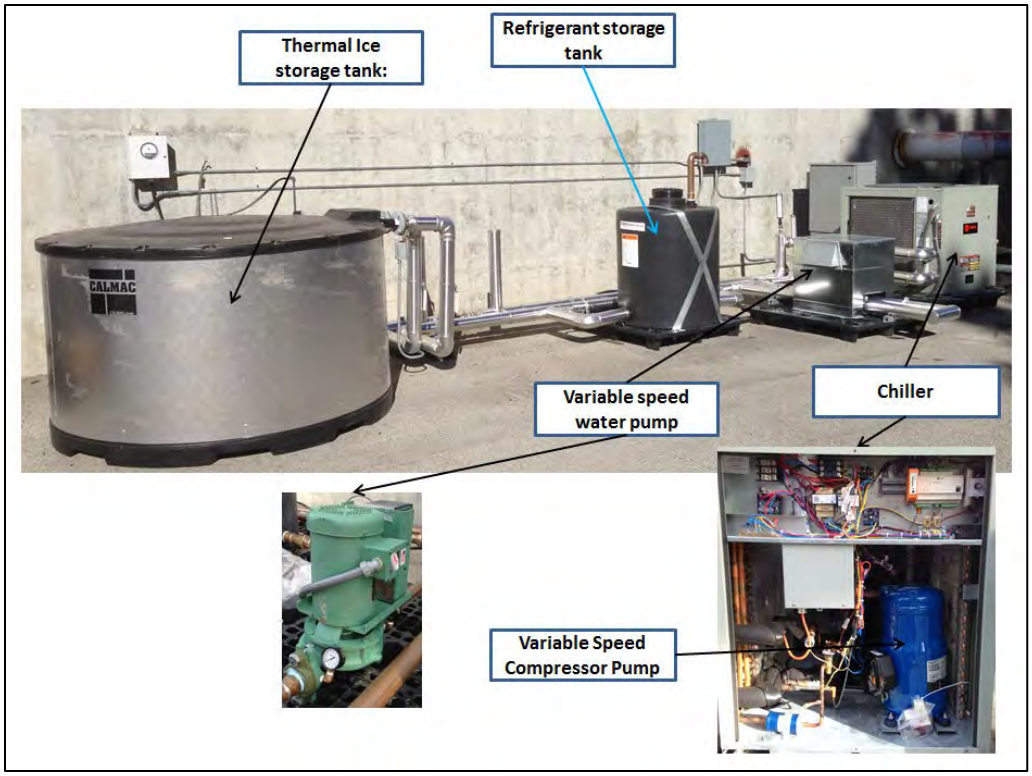

Figure 13. Refrigeration plant for thermal storage.

C. WIND TURBINE SIMULATIONS

In order to measure the expected power output of a three-blade wind turbine, several simulation models were conducted using various blade profiles at varying wind speeds. The simulation results were compared to the experimental results of an actual VAWT called the Mariah Power Windspire at the National Renewable Energy Laboratory's (NREL) National Wind Technology Center (NWTC) located in Golden, Colorado.

The blades used in this project are the 4-digit airfoil profiles developed by National Advisory Committee for Aeronautics (NACA). The first digit represents the maximum camber in a percentage of the chord airfoil length. The next two digits are the position of the maximum camber in tenths of the chord length. The last two digits represent the ratio of the airfoil chord thickness over its length. Figure 14 represents the three different blade profiles used for this project, specifically NACA0012, NACA0015, and NACA0018 profiles [30].

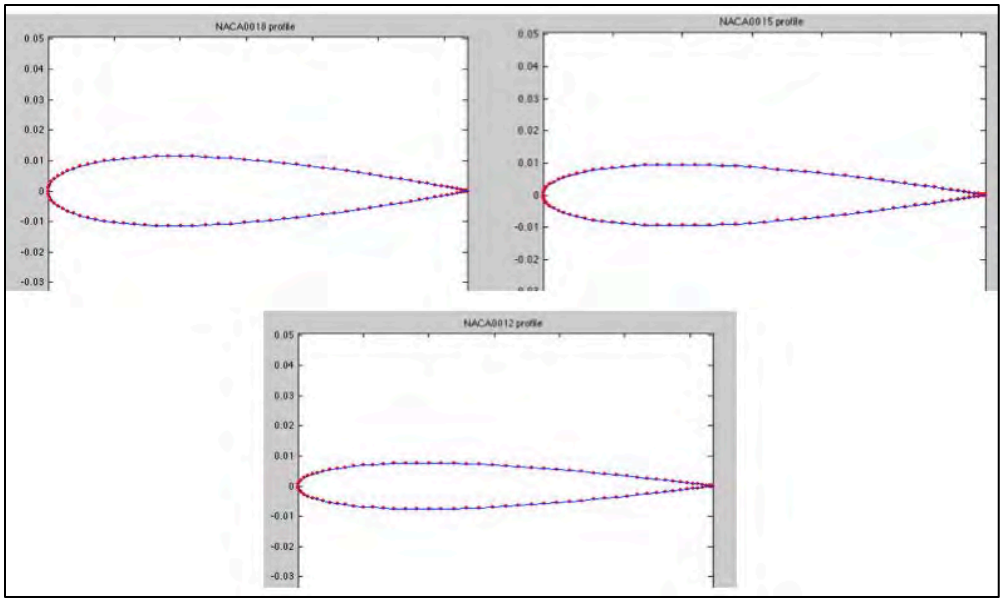

Figure 14. Various blade profiles used for wind turbine simulations.

Solidworks design software helped to create the three-blade profile shown in Figure 15. The radius of the rotor was 0.7 m with the blades located 0.6 m from the center. A separation of 0.1 m of the blade from the rotor's edge incorporate to ensure proper interface between the rotating mesh domain and the stationary mesh domain. The simulation was conducted in a two-dimensional format in order to save computational time and verify that the appropriate blade profile was chosen to closely match the Mariah Windspire wind turbine. The three-blade profile in a rotating mesh spun at various speeds per Table 2.

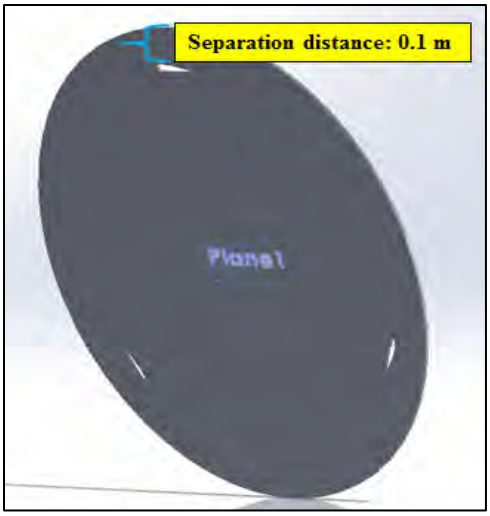

Figure 15. Rotor model created in Solidworks with NACA0018 blade profile.

The static mesh was created to surround the rotating mesh. The size of the static mesh was six times the radius of the rotating mesh to ensure that the air flow from the bottom was fully established prior to interacting with the rotor. The size of the stationary mesh also ensures all the fluctuations due to the interactions between two mesh regions have stabilized prior to exiting the openings. Figure 16 illustrates both the stationary and rotating mesh setup for the simulation. All simulations were conducted with the wind inlet situated at the bottom of the stator. The choice for the wind inlet was determine arbitrary and the resulting torque produced by the blades from the rotating mesh should not be affected by direction of the wind inlet. The left, right, and top of the stationary mesh were all openings with a mass and momentum setting of entrainment and zero relative pressure change.

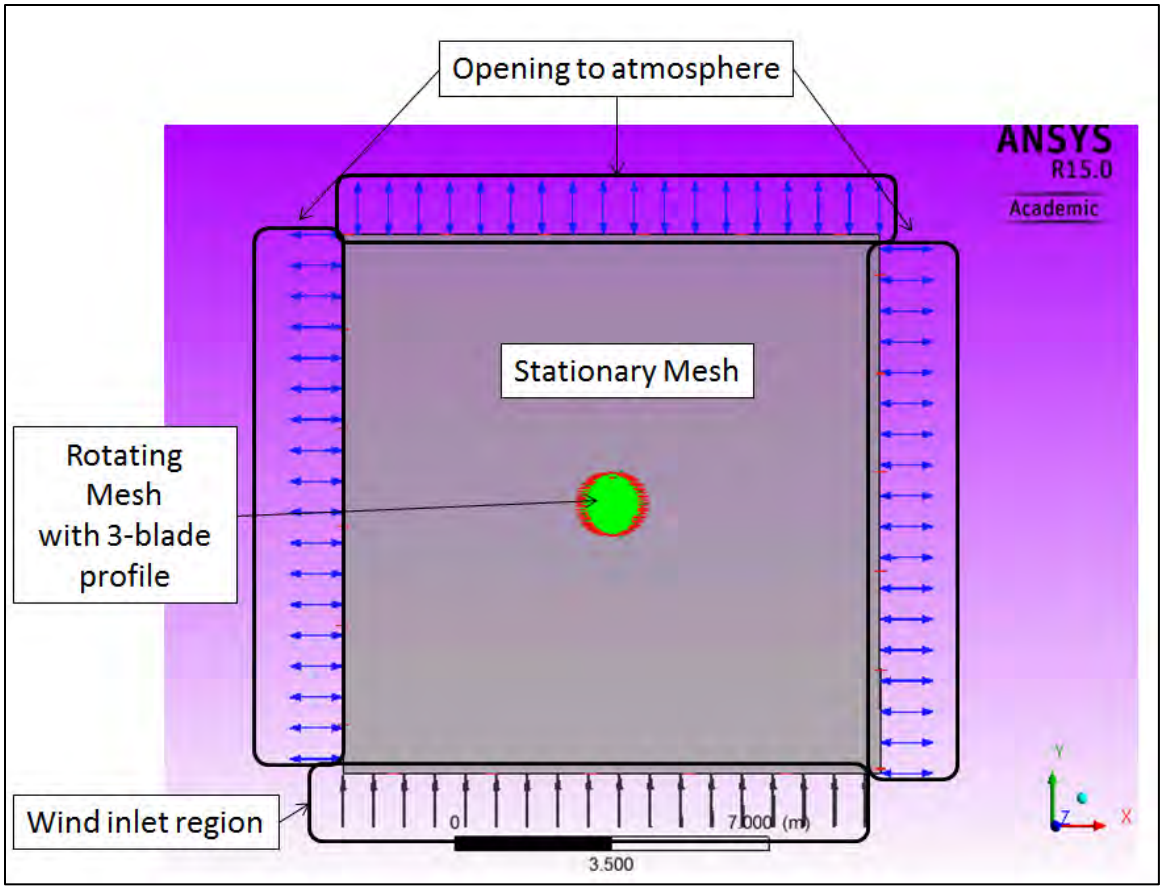

Figure 16. Setup model of the rotor and the stator for simulation.

To obtain a proper level of accuracy, the model was divided into small divisions. The meshing function in ANSYS performed this division. In order to create a 2D modeling, the sweep method was used for both the rotating and stationary mesh using one division along the xy plane. To maximize the number of nodes, edge sizing of 400 divisions were used along the interface of the two mesh regions. The remaining portion of the model was optimized by reducing the normal angle of curvature to 0.20 degrees. The meshing program produced 331,426 nodes with 163,309 elements. The result of the meshing program is shown in Figure 17. Higher node densities near the center region, where the blades were located, are included by the black areas.

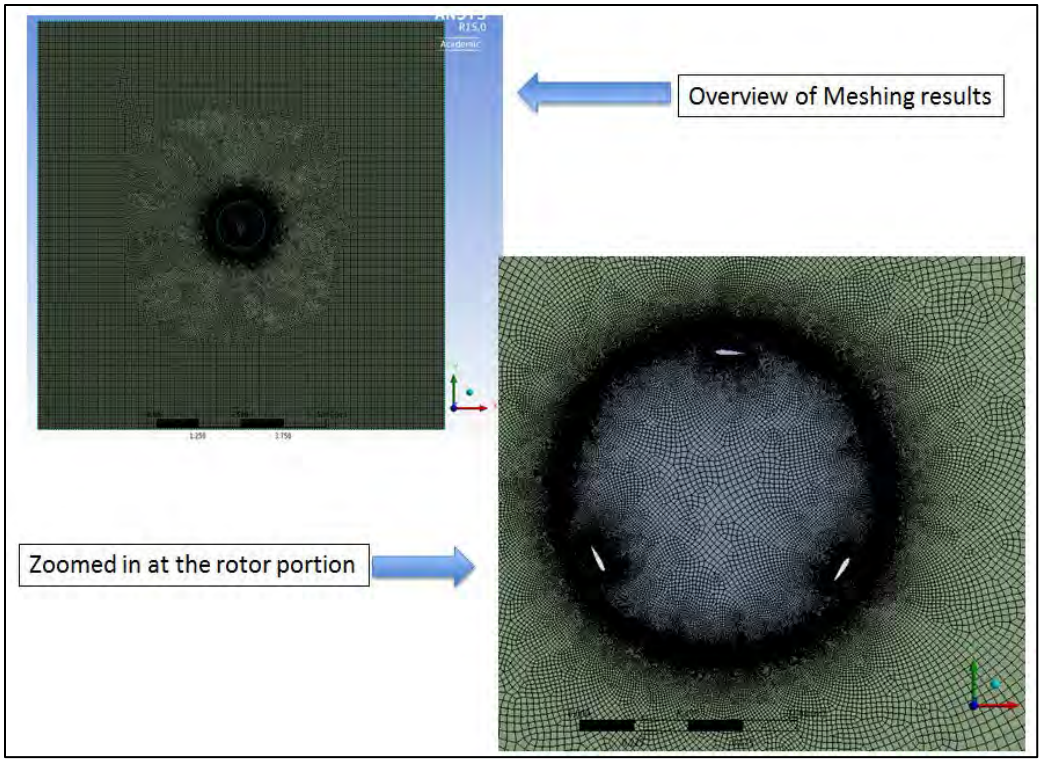

Figure 17. Result of meshing by ANSYS with edge sizing at interface between rotor and stator section.

Table 2 lists the various conditions used for running the simulations. Additionally, the published power coefficient (C_p) and power output in kilowatts (kW) are listed in Table 2 for comparison with simulation results. Only three cases, 1, 4, and 5, were selected for each of the blade profiles due to long computation time required for each simulation run. The length of each of the simulation runs ranged from 30 to over 80 hours. Cases 2 and 3 were additionally run for the NACA0018 blade profile based on its results from cases 1, 4, and 5 closely approximating the experimental results.

Case:	Wind speed [m/s]	Rotation Speed [rev/min]	C_p	Power Output [kW]
1	4	80	0.02	0.01
2	6	228	0.13	0.13
3	8	312	0.18	0.41
4	10	360	0.19	0.88
5	12	346	0.14	1.09

Table 2. Simulation conditions for NACA blade profiles.

The shear stress transport (SST) model and k-epsilon models were both investigated to determine the best turbulence model for the NACA0018 blade profile. SST modeling uses the k-omega model in the inner part of the boundary layer and k-epsilon model in the free-stream [31]. Several more in depth simulation runs were conducted with the NACA0018 profile. Specifically, several additional wind speeds and two turbulence model were examined for the NACA0018 profile. Table 3 illustrates a list of the additional conditions used to evaluate the NACA0018 profile. The 11 m/s and 13 m/s wind speeds were used to verify that there is a reduction in power when the wind speed is greater than 12 m/s.

Case:	Wind Speed [m/s]	Rotor Speed [rev/min]	C_p	Power [kW]
1	4	80	0.02	0.01
2	6	228	0.13	0.13
3	8	312	0.18	0.41
4	10	360	0.19	0.88
5	11	352	0.17	1.02
6	12	346	0.14	1.09
7	13	318	0.1	0.96

Table 3. NACA0018 simulation condition used for turbulence modeling comparison.

Two main relationships used are C_p and power output (P). C_p shows the relationship of the power extracted by the wind turbine to the wind energy available. To determine the power output, a monitor point was defined in setup model for the torque at the blades. With the torque (T) value known, power can be calculated as follows:

$$P = T\omega;$$

where, T is the average torque in joules or N-m determined from ANSYS modeling and ω is the angular velocity in radians per second.

III. OBSERVATION AND RESULTS

A. EQUIPMENT RESULTS

The alternating current (AC) produced by the wind turbines from August 2014 through October 2014 varied greatly. Table 4 shows the power production statistics over the past three months. The VAWTs continued to produce electricity for up to 10 minutes due to their size. This is significant because the minimum run time for the refrigeration plant's compressor pump to run is 10 minutes. Based on the designed control algorithm—which detects for five continuous-frequency AC power-readings prior to initiating the start-up sequence—there should be sufficient power available to complete the process without needing to draw from either the batteries or the main grid. Table 4 illustrates that statics of the single-run continuous power production of the wind turbines.

Single-run Continuous Power Production Time Statistics		
Average Power Production Time:	37.4	Minutes
Minimum Power Production Time:	10.0	Minutes
Maximum Power Production Time:	143.3	Minutes

Table 4. Power production statistics during the monitor period of August to October 2014.

During the three months of data collection, the duration of power production from the VAWTs varied significantly, as shown in Figure 18. This figure shows that the maximum amount of time that power was generated during any given week was approximately 450 minutes.

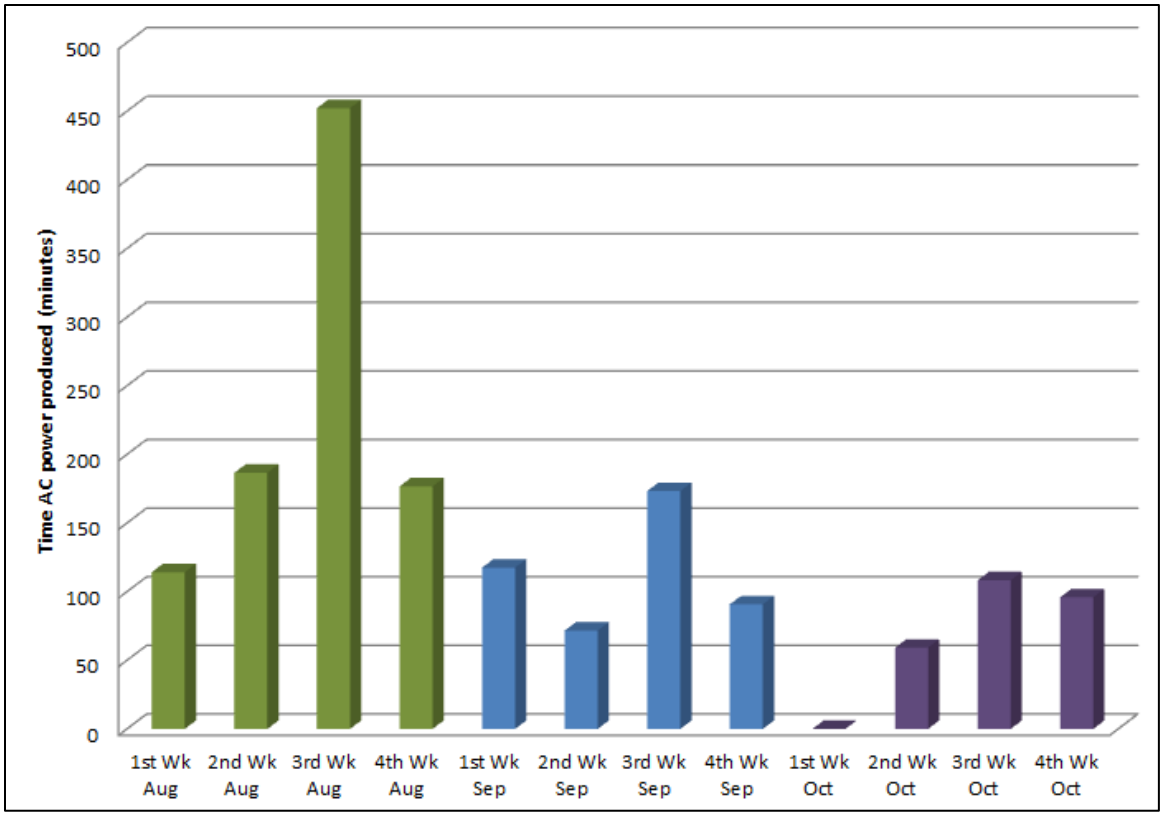

Figure 18. Weekly Alternating Current Production by the UGE Visionaire5 vertical axis wind turbines at the Turbopropulsion Laboratory. Data collected during the months of August through October 2014.

Figure 19 provides a broader view of this data. This figure compares the data for the entire month. The general trend during this three-month period, from summer into fall, is that wind power steadily declines.

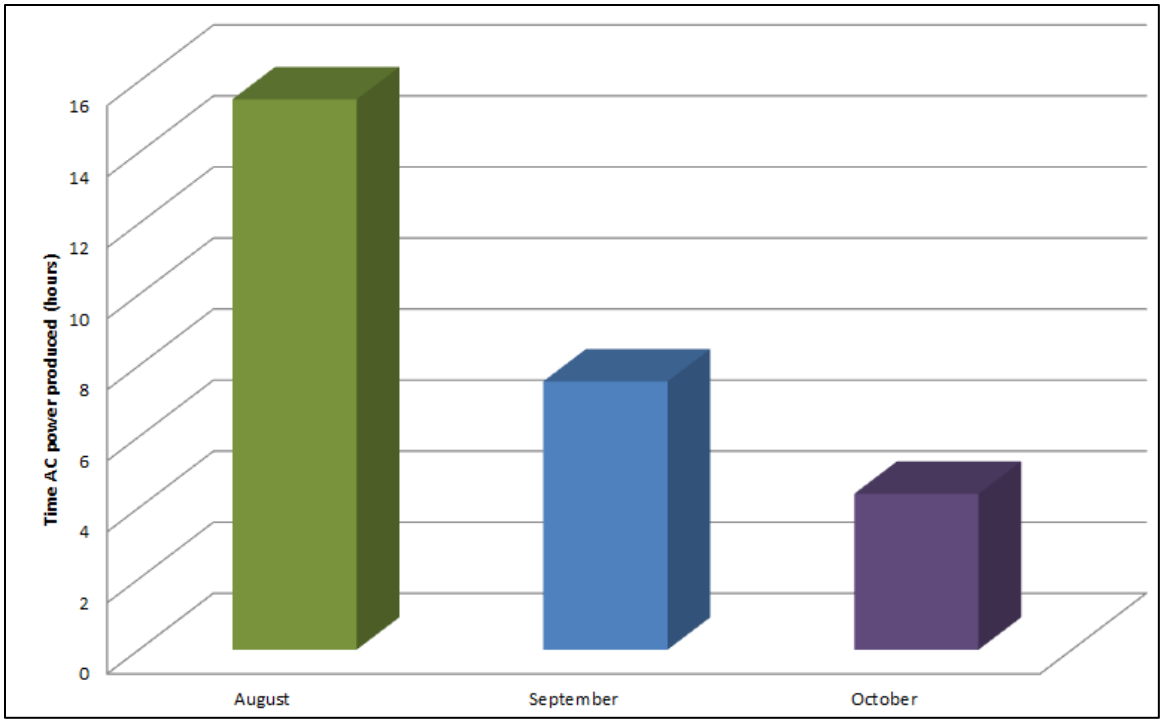

Figure 19. Hours of alternating current production during the three months monitoring period at the Turbopropulsion Laboratory.

The VAWTs produced power for approximately one percent of the time during the data collection period. Due to a short sample duration, the results variation appears to be fairly large. As more data is collected in future projects, AC power production by the VAWTs can be more thoroughly analyzed.

Based on the results of this research, AC power production by the VAWTs is indeed possible. Unfortunately, the only electrical load was the battery during the research time span. The master Sunny Island kept the battery state on a float charge; that is, the battery is charging at a rate that is close to the rate of discharge. This means that the battery state of charge is always close to 100 percent. Thus, when wind produced power, there was no place to store or use it, which was a majority of the time. The installation time for the variable power refrigeration plant took longer than expected and due to some scheduling conflicts, the control program for the refrigeration did not occur.

B. WIND TURBINE SIMULATION RESULTS

Figure 20 depicts the result of the wind turbine simulation runs of the three NACA blade profiles for power output (kW) versus wind speed (m/s). NACA0018 provides the best results for comparison with the experimental data. NACA0012 and NACA0015 blade profiles produced less power for the 10 m/s and 12 m/s wind speeds than observed in the experiments.

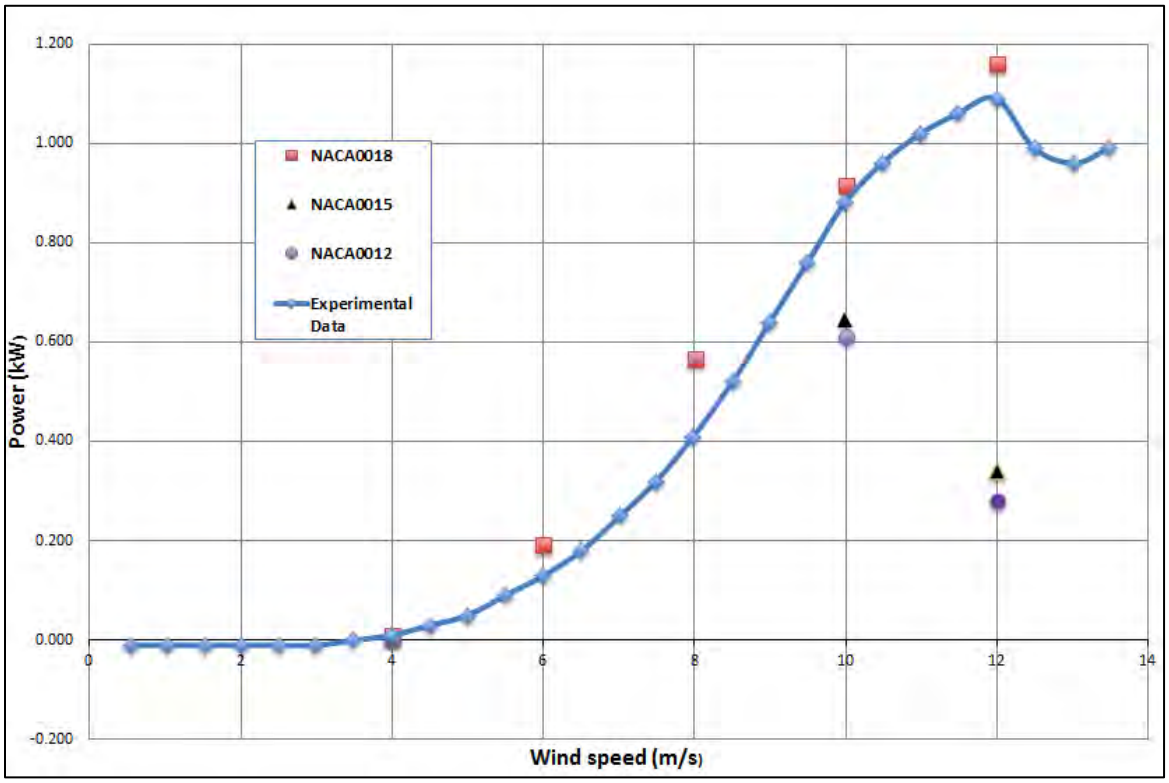

Figure 20. Power versus Wind speed for various NACA blade profiles.

A comparison of the simulation and the experimental data for C_p versus wind speeds is shown in Figure 21. The NACA0018 blade profile provided the best matching c_p compared to the other two blade profiles. Based on the results of Figure 20 and 21, further investigation was conducted on the NACA0018 profile.

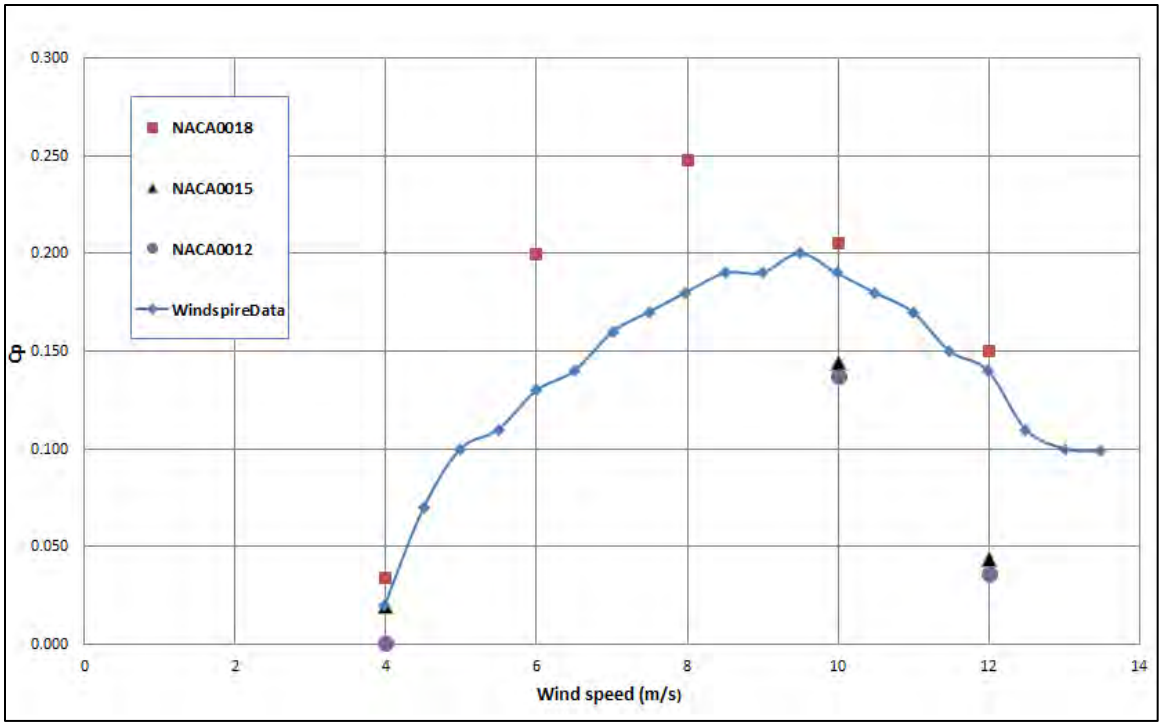

Figure 21. C_p versus wind speeds for various NACA blade profiles.

An in-depth examination was conducted on the NACA0018 profile using additional wind speeds and two different turbulence models. Figure 22 shows the power versus wind speed for the NACA0018 profile with a comparison of SST and the K-epsilon turbulence models. At wind speeds of less than or equal to 10 m/s, the SST turbulence model provided the more accurate prediction of power output for the wind turbine. However, when the wind speed was greater than 10 m/s, the K-epsilon turbulence model provided a closer trend prediction. Both turbulence models did show a reduction in power after reaching a maximum wind speed of 10 m/s and 11 m/s for the SST and K-epsilon models, respectively. This highlights the difficulty that turbulence models have simulating transient and separated flows such as those found in vertical axis wind turbines.

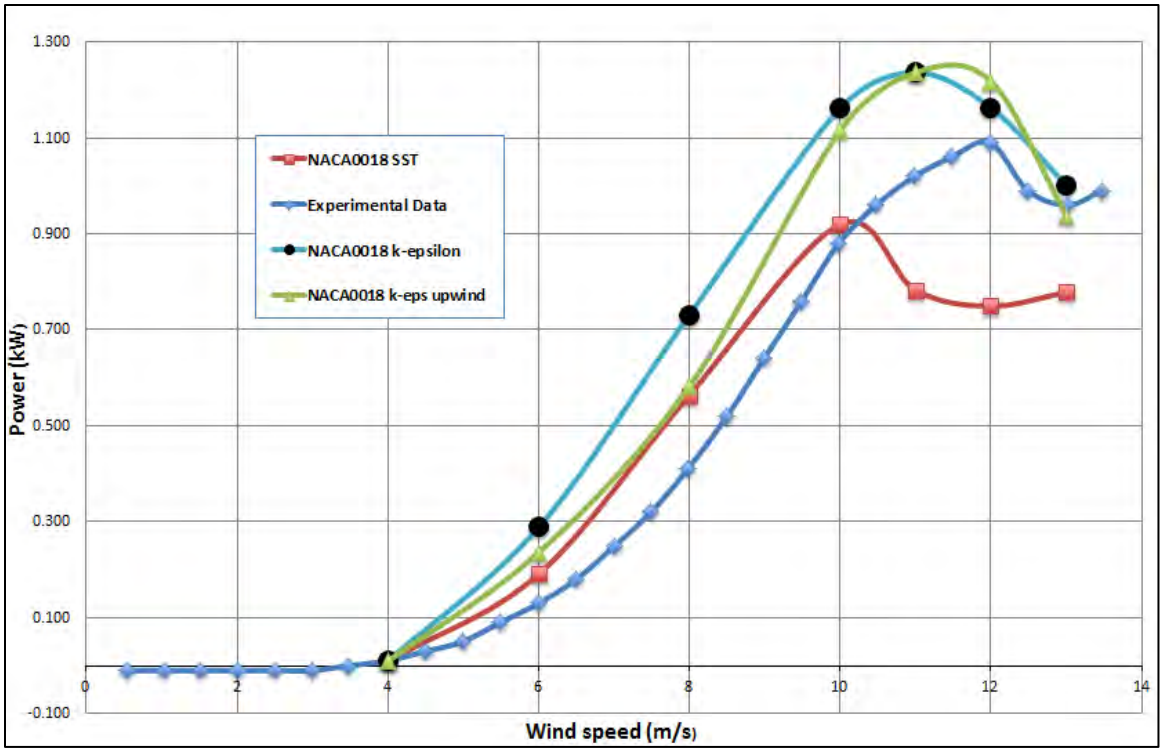

Figure 22. Power versus wind speed for NACA0018 profile with a comparison of SST and K-epsilon turbulence model.

In examining the power coefficient versus wind speed plot in Figure 23, the SST model provided better correlation with wind speeds of less than or equal to 10 m/s. This aligned closely with the result shown in Figure 22. Furthermore, when the wind speed was greater than 10 m/s, the k-epsilon model closer predicted C_p to the experimental results, similar to Figure 22.

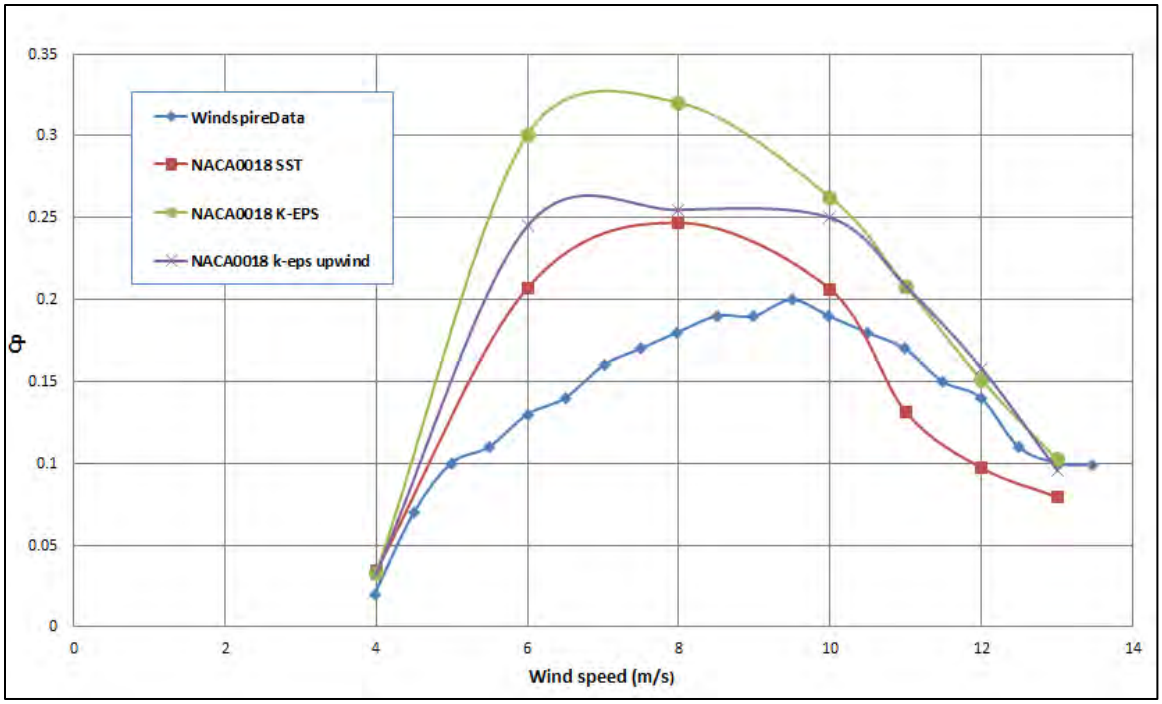

Figure 23. C_p versus wind speed for NACA0018 profile comparison of SST and k-epsilon turbulence model.

The results of the simulation illustrates that the NACA0018 blade profile closely matched the published experimental results. Further simulations demonstrated that the wind speeds play a factor in selecting the appropriate turbulence modeling.

THIS PAGE INTENTIONALLY LEFT BLANK

IV. CONCLUSION

The goal of this thesis was to commission a renewable powered micro-grid and to collect production data from two vertical axis wind turbines (VAWTs). This thesis initiated the design for the controlling the power supply sequences for the variable power refrigeration plant.

One VAWT produced power over a period of three months. Although the length of time power production only accounted for approximately one percent of the monitored time, the single-run continuous power lasted on average over 37 minutes, with a minimum time of ten minutes. Hence, to answer the research question, the conditions at TPL are indeed feasible for operating a variable speed refrigeration plant. However, the amount of ice produced by the refrigeration plant would likely be small, due to the short length of time that wind energy is available at the TPL. This research was not able to analyze load matching of the refrigeration plant to incoming renewable energy due to the delay in refrigeration plant installation.

In line with the ESTEP philosophy, this research has demonstrated that it was possible to used COTS components to establish a micro-grid at the TPL. For cooling, a thermal ice storage system is a viable option. A zero-to-ten VDC has been outputted to the variable speed chiller plant to produce ice. Based on initial runs of the chiller plant, the power drawn from the battery has been minimal. Hence, if power from renewable energy source is lost during the initial start-up of the chiller plant, the battery can support the ten-minute initial lubrication period required for chiller operation.

This thesis also verified published experimental data of a three-blade VAWT. The first step of the simulation determined that the NACA0018 blade profile matched the National Renewable Laboratory's Mariah Power Windspire published results. The second step examined the SST and k-epsilon turbulence models. The results showed that at lower wind speeds, less than ten miles per hour, the SST provided the best correlation with the results. As the wind speeds increased to greater than ten miles per hour, the k-epsilon model provided a more accurate reading.

THIS PAGE INTENTIONALLY LEFT BLANK

V. RECOMMENDATIONS

While this research programmed and monitored the micro-grid system with wind energy, continuation of the program requires further refinement. There are four recommendations for future research:

1. Install additional renewable energy collection systems to ensure sufficient power collection,
2. Implement established control system design to operate the variable power refrigeration plant,
3. Examine an alternative thermal storage system for other uses such as heating,
4. Reconfigure the micro-grid for optimal performance and energy storage after all components have operated as an integral system.

To improve collection ability, solar thermal and photovoltaic cells should be installed to provide greater renewable energy collection ability. The cells should be tied to the micro-grid to increase the amount of power production. The preliminary integrated system design shown in Figure 7 illustrates the approximate location of these cells. To ensure maximum sunlight collection, the cells should be mounted on the south side of building 216 at the TPL.

Future micro-grid design must take into account the ease of controllability. A simpler controller architecture would be desirable to more easily manage each of the subsystems.

Heating and cooling of facilities are significant users of energy. An examination of thermal storage in bricks would provide more flexibility for energy storage and future usage. Bricks could be an option for heating a building during the winter.

Consideration should be made in the future after several years of collecting performance data on the wind turbines to change its position on top of the building. Recently, an anemometer was purchased and received at the TPL. This should assist in determining the optimal location of the turbines to collect wind energy. Another

possibility for reconfiguring the micro-grid would be to replace the batteries with super-capacitors. Super-capacitors have larger life-cycles than batteries and higher power densities [32].

APPENDIX A. COMMISSIONING OF THE SUNNY WEB BOX PROCEDURE

These steps were taken to commission the first Web Box. The Web Box monitors the information coming from the SUNNY Island, which measures the power output from the micro-grid.

5. The Web Box needs to be connected by an Ethernet cable to either a hub or to a computer.

6. Using the SMA-Installation Disk, run the SUNNY-WebBox-Assistant.exe file. This will start the SUNNY Web Box Assistant (SWBA).

7. Accept the license agreement and click Next.

8. Power on the Web Box by connecting the power cord to an outlet. This usually takes about 90 seconds to completely power on.

9. Ensure the box is checked for "The SUNNY Webbox Assistant to start search for SUNNY Webbox."

10. The following steps are taken with the SWBA:

    a. Installation type: select →Integrate the 1st SUNNY Webbox in the Photo Voltaic (PV) system and click Next.

    b. Select configure SUNNY Web Box manually and click Next.

    c. Edit the system settings by clicking Edit

        i) Name of Plant Operator: Windy1
        ii) System Name: Garth
        iii) Time setting: verify correct time and click Next.
        iv) Select static network setting for local network. **DO NOT** connect to the NPS network without Information Technology and Communications Services (ITACS) approval.
        v) Check the box for "Your computer is in the same network into which the SUNNY Webbox shall be integrated."
        vi) For external communications (per reference AA1, this is not important because there are no external communication taking place for the Web Box), the following are inputted
        vii) DNS Server IP: 192.168.0.1;
        viii) Gateway IP: 192.168.0.1;
            a. IP Address (automatically assigned): 192.168.0.168;

b. Subnet mask (automatically assigned): 255.255.255.0 and click Save.

11. Data Setting: uncheck the box for use SUNNY portal since the Web Box will not be connected to the Internet. Check the second box for "Do you wish to use the integrated FTP server or an SD Card?" It is important to check the second box otherwise; the SD card slot will be disabled.

APPENDIX B. START-UP AND SHUTDOWN PROCEDURE FOR THE MICRO-GRID AT TPL

1. Start-up Procedure

The following procedure is provided for the startup of the micro-grid at building 216 of the TPL at NPS.

1. Supply power from the main grid to the micro-grid by closing the main terminals in breaker box. The breaker box is located along the south side of building 216 approximately three quarters of the way inside the entrance. The break box is labeled "POWER PANEL LP-G" with the breaker numbers of 8, 10, and 12.

2. Starting with the Sunny Island (SI) on the farthest right, turn-on the SI by switching the DC circuit breaker of the SI to "ON," SI number 1 as shown on Figure B1. Once turned on, SI display will read "Ready….Waiting for Master."

3. Repeat step 2 for the center SI number 2 on the Figure B1.

4. The master SI number 3, which is located on the farthest left when facing the panel as shown in Figure B1, should be started last. Once the master SI is turned on, it will be in stand-by mode (STBY). Then, the display on the master SI will be ready, and read "STNDBY: To Start INV hold <ENTER>."

5. Press and hold <ENTER> on the master SI until the horizontal bar disappear and 3 beeps are heard.

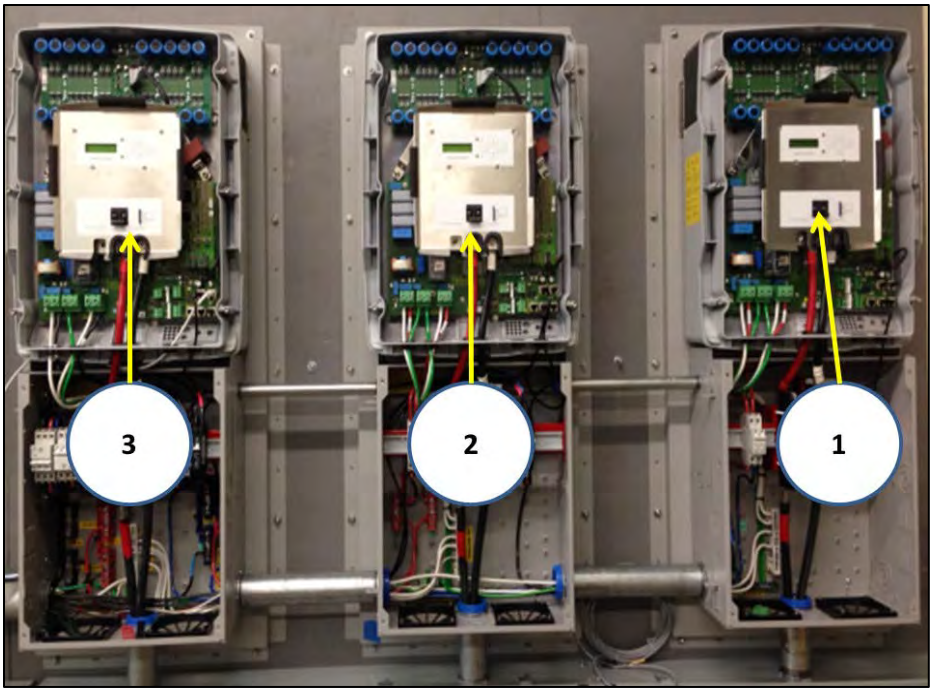

Figure B1. Order for starting up the SUNNY Island inverters.

6. The SI will take approximately five minutes to charge up and display the correct voltage from the main grid of approximately 203 V.

The following procedure is provided for the normal shutdown of the micro-grid at building 216 of the Turbo propulsion laboratory at Naval Postgraduate School (NPS).

2. Shutdown Procedure

Initial condition: the SI inverters are in normal operation mode.

1. Starting with the master SI, SI number 3 on Figure B1, hold down the <ESC> button until the vertical bar disappears to shift from operations mode to stand-by (STANBY) mode. The SI display should read, "STNDBY: To Start INV hold <ENTER>."

2. Repeat step 1 for SI number 2 and 1 on Figure B1. This will place all three of the SI in STNDBY mode.

3. Starting with the Master SI number 3, turn off the SI by switching the DC breakers to "OFF" position. Then turn off the breakers for the remainder the SI.

APPENDIX C. ELECTRICAL DRAWINGS OF THE MICRO-GRID PROVIDED BY NEXGEN

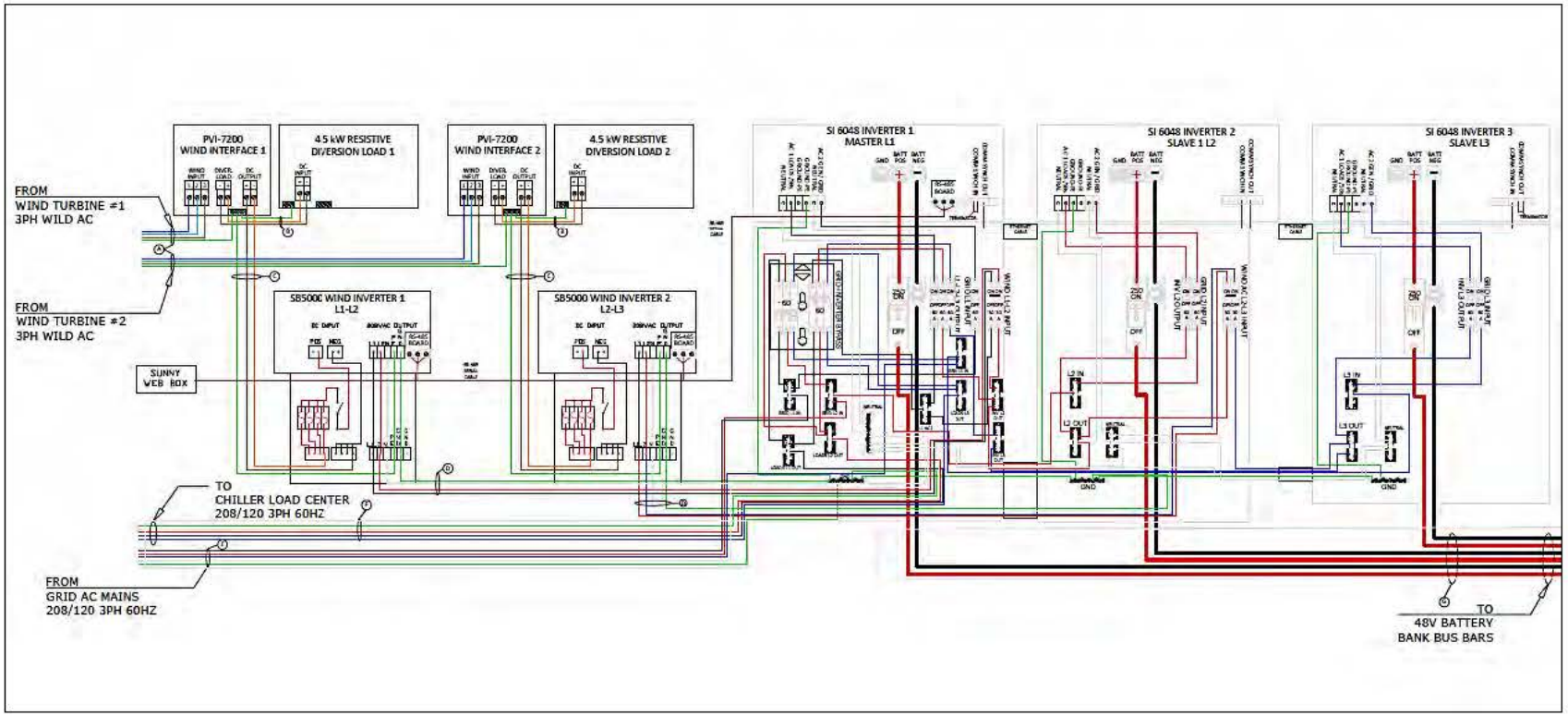

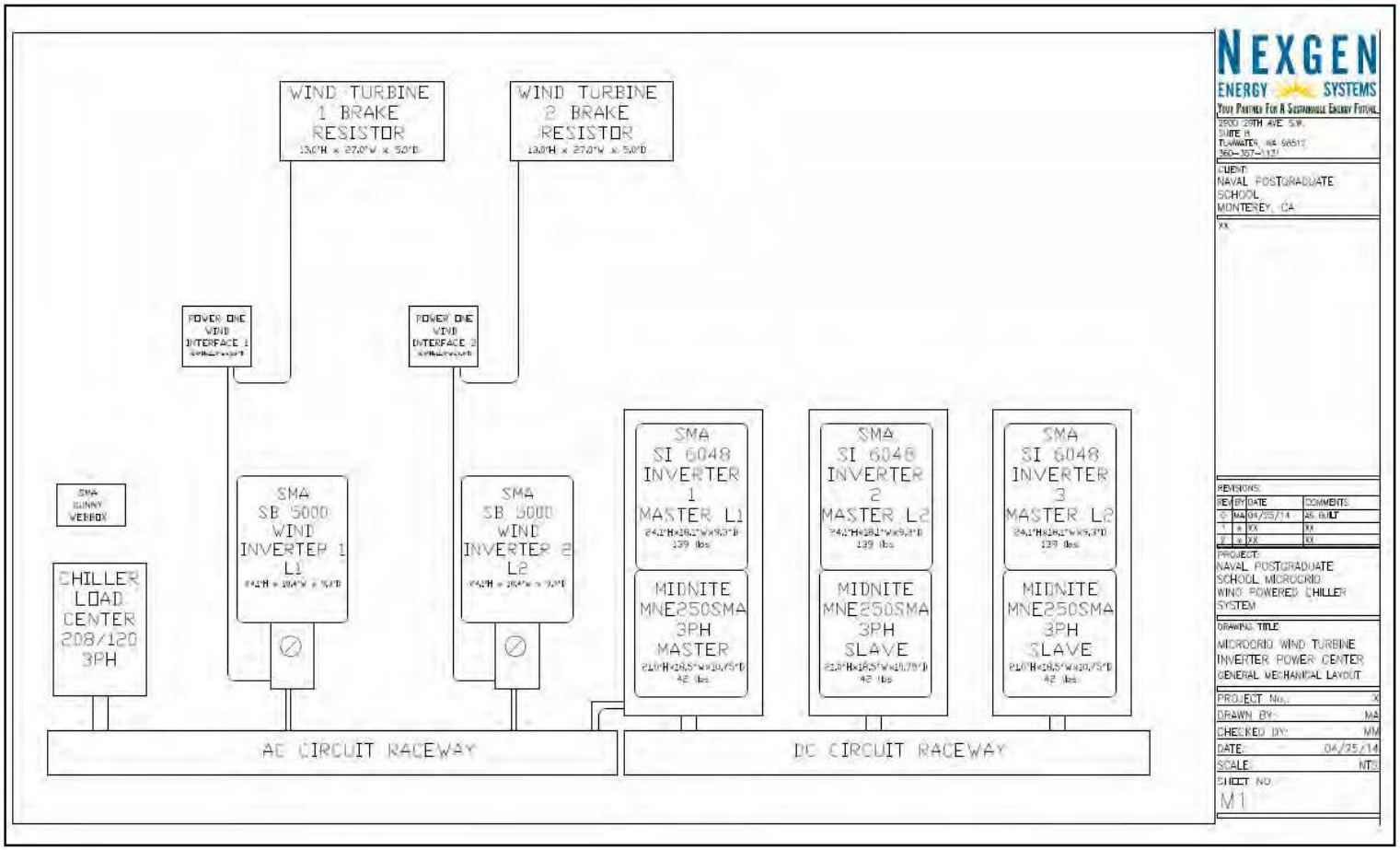
WIND TURBINE 1 BRAKE RESISTOR
WIND TURBINE 2 BRAKE RESISTOR
POWER ONE WIND INTERFACE 1
POWER ONE WIND INTERFACE 2
SMA SUNNY VEBBOX
CHILLER LOAD CENTER 208/120 3PH
SMA SB 5000 WIND INVERTER 1 L1
SMA SB 5000 WIND INVERTER 2 L2
SMA SI 6048 INVERTER 1 MASTER L1
MIDNITE MNE250SMA 3PH MASTER
SMA SI 6048 INVERTER 2 MASTER L2
MIDNITE MNE250SMA 3PH SLAVE
SMA SI 6048 INVERTER 3 MASTER L2
MIDNITE MNE250SMA 3PH SLAVE
AC CIRCUIT RACEWAY
DC CIRCUIT RACEWAY
NEXGEN ENERGY SYSTEMS
YOUR PARTNER FOR A SUSTAINABLE ENERGY FUTURE
2800 28TH AVE S.W.
SUITE B
TUMWATER, WA 98512
360-357-5131
CLIENT:
NAVAL POSTGRADUATE SCHOOL
MONTEREY, CA
XX
REVISIONS:
REV BY DATE COMMENTS
0 MA 04/25/14 AS-BUILT
1 x XX XX
2 x XX XX
PROJECT:
NAVAL POSTGRADUATE SCHOOL MICROGRID WIND POWERED CHILLER SYSTEM
DRAWING TITLE:
MICROGRID WIND TURBINE INVERTER POWER CENTER GENERAL MECHANICAL LAYOUT
PROJECT No.: X
DRAWN BY: MA
CHECKED BY: MM
DATE: 04/25/14
SCALE: NTS
SHEET NO.
M1

APPENDIX D. CFD SIMULATION SETTINGS FOR WINDSPIRE ANALYSIS

Analysis Type	Basic Settings • External Solver Coupling o Option • Analysis Type o Option • Time Duration o Option o Timesteps per Run • Time Steps o Option o Timesteps • Initial Time o Option o Time	 None Transient Total Time 2 [s] Timesteps 0.0005 [s] Automatic with value 0 [s]
Rotor Domain	Basic Settings • Location & Type o Location o Domain Type o Coordinate Frame • Fluid and Particle Definitions o Fluid 1 ▪ Option ▪ Material ▪ Morphology • Option ▪ Minimum Volume Fraction • Domain Models o Pressure ▪ Reference Pressure o Buoyancy Model ▪ Option o Domain Motion ▪ Option ▪ Angular Velocity ▪ Alternate Rotation Model ▪ Axis Definition • Option • Rotation Axis ▪ Mesh Deformation Fluid Models • Heat Transfer o Option o Incl. Viscous Work Term	 B14 Fluid Domain Coord 0 Material Library Air Ideal gas Continuous Fluid Unchecked 1 [atm] Non Buoyant Rotating 360 [rev min^-1] Unchecked Coordinate Axis Global Z None Total Energy Unchecked

	• Turbulence o Option o Wall Function o High Speed (compressible) Wall Heat Transfer Model o Turbulent Flux Closure for Heat Transfer • Advanced Turbulence Control • Combustion o Option • Thermal Radiation o Option • Electromagnetic Model Initialization • Domain Initialization o Frame Type o Coordinate Frame • Initial Conditions o Velocity Type o Cartesian Velocity Components ▪ Option ▪ U ▪ V ▪ W o Static Pressure ▪ Option ▪ Relative Pressure o Temperature ▪ Option ▪ Temperature o Turbulence ▪ Option	k-Epsilon Scalable Unchecked Unchecked Unchecked None None Unchecked Checked Stationary Unchecked Cartesian Automatic with Value 0 [m s^-1] 10 [m s^-1] 0 [m s^-1] Automatic with Value 0 [atm] Automatic with Value 288.15 [K] Medium (Intensity = 5%)
Stator Domain	Basic Settings • Location & Type o Location o Domain Type o Coordinate Frame • Fluid and Particle Definitions o Fluid 1 ▪ Option ▪ Material ▪ Morphology • Option ▪ Minimum Volume Fraction • Domain Models o Pressure	 B35 Fluid Domain Coord 0 Material Library Air Ideal gas Continuous Fluid Unchecked 1 [atm]

	▪ Reference Pressure o Buoyancy Model ▪ Option o Domain Motion ▪ Option o Mesh Deformation ▪ Option Fluid Models • Heat Transfer o Option o Incl. Viscous Work Term • Turbulence o Option o Wall Function o High Speed (compressible) Wall Heat Transfer Model o Turbulent Flux Closure for Heat Transfer • Advanced Turbulence Control • Combustion o Option • Thermal Radiation o Option • Electromagnetic Model Initialization • Domain Initialization o Frame Type o Coordinate Frame • Initial Conditions o Velocity Type o Cartesian Velocity Components ▪ Option ▪ U ▪ V ▪ W o Static Pressure ▪ Option ▪ Relative Pressure o Temperature ▪ Option ▪ Temperature o Turbulence Option	Non Buoyant Stationary None Total Energy Unchecked k-Epsilon Scalable Unchecked Unchecked Unchecked None None Unchecked Checked Stationary Unchecked Cartesian Automatic with Value 0 [m s^-1] 10 [m s^-1] 0 [m s^-1] Automatic with Value 0 [atm] Automatic with Value 288.15 [K] Medium (Intensity = 5%)
Default Fluid-Fluid Interface	Basic Settings • Interface Type o Interface Side 1	Fluid-Fluid Rotor

	▪ Domain (Filter) ▪ Region List o Interface Side 2 ▪ Domain (Filter) ▪ Region List o Interface Models ▪ Option ▪ Frame Change/Mixing Model • Option ▪ Pitch Change • Option Additional Interface Models • Mass And Momentum o Option o Interface Model ▪ Option o Conditional Connection Control Mesh Connection • Mesh Connection Method o Mesh Connection ▪ Option • Intersection Control	F18.14 Stator F42.35 General Connection Transient Rotor Stator Automatic Conservative Interface Flux None Unchecked GGI Unchecked
Solver: Solution Units	Basic Settings • Mass Units • Length Units • Time Units • Temperature Units • Angle Units o Angle Units • Solid Angle Units o Solid Angle Units	 [kg] [m] [s] [K] Checked [rad] Checked [sr]
Solver: Solver Control	Basic Settings • Advection Scheme o Option • Transient Scheme o Option o Timestep Initialization ▪ Option ▪ Lower Courant Number ▪ Upper Courant Number • Turbulence Numerics o Option • Convergence Control o Min. Coeff. Loops o Max. Coeff. Loops o Fluid Timescale Control ▪ Timescale Control • Convergence Criteria	 High Resolution Second Order Backward Euler Automatic Unchecked Unchecked First Order 1 4 Coefficient Loops

	o Residual Type o Residual Target o Conservation Target • Elapsed Wall Clock Time Control • Interruption Control Equation Class Settings • Equation Class o Energy ▪ Advection Scheme • Option o Transient Scheme Advanced Options • Pressure Level Information • Body Forces • Interpolation Scheme • Temperature Damping • Velocity Pressure Coupling • Compressibility Control o High Speed Numerics o Total Pressure Option o Clip Pressure for Properties ▪ Minimum Pressure for Properties • Intersection Control	RMS 1.E-4 Unchecked Unchecked Unchecked Energy Checked Checked Upwind Unchecked Unchecked Unchecked Unchecked Unchecked Unchecked Checked Checked Unchecked Unchecked Unchecked Unchecked
Solver: Output Control	Results • Option • File Compression • Output Equation Residuals • Extra Output Variables List Backup • Backup Results Trn Results • Transient Results o Transient Results 1 ▪ Option ▪ File Compression ▪ Output Equation Residuals ▪ Extra Output Variables List ▪ Output Frequency • Option • Timestep Interval Trn Stats • Transient Statistics Monitor • Monitor Objects o Monitor Coefficient Loop Convergence o Monitor Balances - Full o Monitor Forces - Full	 Standard Default Unchecked Unchecked None Transient Results 1 Standard Default Unchecked Unchecked Timestep Interval 50 None Checked Unchecked

	o Monitor Residuals - Full o Monitor Totals - Full o Monitor Particles - Full o Monitor Points and Expressions ▪ Torquez • Option • Expression Value • Coordinate Frame Export • Export Results	 Torquez Expression torque_z()@Rotor Default Coord 0 None
Solver: Expert Parameters	Convergence Control • High Speed Models o Max continuity loops o Value	 Checked 3

APPENDIX E. MATLAB CODE FOR CREATING THE 3-BLADE ROTOR

```
%------------------
%
%   VAWT Blade profile NACA00XX
%
%------------------

% 3-Blade Vertical Axis Wind Turbine Builder Program
% Written by CDR Rex Boonyobhas with advise from Dr. Garth Hobson and
% Dr. Anthony Gannon
%
% This MATLAB program will request for input the NACA00XX Airfoil
% profile
% from the user, the angle of attack, the chord length, the radius of
% the rotor, and the number of points desired to make up the blade
% profile.
% The program outputs the plot of the original blade profile and the
% blade profile based on the angle of attack. Additionally, the       %
program will initialize Solidworks to create a 3-blade rotor with a  %
thickness of 1.0 millimeter.
%
% Variable identification:
% alpha:    Angle of attack in degrees
% tau:      Last two digits of the NACA00XX profile
% cord:     Chord length
% n_blades: Number of blades for the rotor
% m:        Thickness of the rotor
% radius:   Radius of the rotor

clear all;
close all;
clc;

alpha = input('Angle of attack in degrees ')
if isempty(alpha)
   alpha = 0.0
end
alpha_deg=alpha
alpha=alpha*pi/180.0;
%
% NACA 00xx thickness
%

tau = input('Percent Thickness of a NACA 4-digit Airfoil, eg. NACA0012
type 12')
if isempty(tau)
   tau = 18 % Default is NACA0018 Airfoil
end
%
% Chord
```

```
%
cord = input('Chord Length')
if isempty(cord)
   cord = 0.127
end
thickness = cord*tau;
n_blades = 3;
s_thick  = 0.01;  %Slice thickness in meters

% No. of points around the airfoil
m = input('No. of points around the airfoil')
if isempty(m)
   m = 100
end

% Inputting radius
radius = input('Input the radius of the rotor[m]: ')
if isempty(radius)
   radius = 0.6
end

md2=m/2;
delt=pi/md2;
for i=1:md2+1
    theta(i)=delt*(i-1);
    x(i)=0.5*(1.0+cos(theta(i)));
    y(i)=-5*(tau/100)*cord*(0.2969*sqrt(x(i))-...
    0.126*(x(i))-0.3537*(x(i))^2+...
    0.2843*(x(i))^3-0.1015*(x(i))^4);
    x(i)=x(i)*cord;
end

for i=md2+2:m+1
    theta(i)=delt*(i-(md2+1));
    x(i)=0.5*(1.0-cos(theta(i)));
    y(i)=5*(tau/100)*cord*(0.2969*sqrt(x(i))-...
    0.126*(x(i))-0.3537*(x(i))^2+...
    0.2843*(x(i))^3-0.1015*(x(i))^4);
    x(i)=x(i)*cord;
end

plot(x,y,'r.')
title(['NACA00',num2str(tau),' profile'])
axis([0 cord -0.4*cord 0.4*cord])
grid on

%
%   Rotate the airfoil
%

for i=1:m+1
    X(i) = x(i)*cos(alpha)+y(i)*sin(alpha);
    Y(i) = x(i)*sin(alpha)-y(i)*cos(alpha);
end
```

```
hold on
plot(X,Y,'b')

%
%   Translate
%

DELX = 0.25*cord
DELY = .61

for i=1:m+1
    XX(i) = (X(i)-DELX);
    YY(i) = (Y(i)+DELY);
    ZZ(i) = 0;
end

figure(2)
plot(XX,YY,'b')
title(['NACA00',num2str(tau),' profile - Rotated & Translated'])
axis([-0.2*DELY DELY 0 1.2*DELY])
grid on

xyz=[XX;YY]';
xyz(:,3)=0;
xyz

Coxyz = fopen('coorxyz.txt','w');
fprintf(Coxyz,'%2.10f %2.10f %2.10f\n', [XX;YY;ZZ]);
fclose(Coxyz);
type coorxyz.txt

%%
% Start solidworks and close all open SolidWorks files
NET.addAssembly('C:\Program Files\SolidWorks Corp\SolidWorks
(2)\SolidWorks.Interop.sldworks.dll'); % interop services file
swApp = SolidWorks.Interop.sldworks.SldWorksClass; % Create Solidworks
app in
swApp.CloseAllDocuments(true);

% Make application visible
if ~(swApp.Visible)
    swApp.Visible = true;
end

% Template with SI units is opened
Part  = swApp.OpenDoc6([pwd '\Template.SLDPRT'], 1, 0, [], 0,0);

%This allows geometries of less than 1mm
Part.SketchManager.AddToDB = true;
Part.SketchManager.DisplayWhenAdded = false;

%Draw Circle
```

```
Part.Extension.SelectByID2('Front Plane', 'PLANE', 0, 0, 0, false, 0,
[], 0);
Part.SketchManager.InsertSketch(true)
Part.SketchManager.CreateCircle(0, 0, 0, radius, 0, 0);
Part.SketchManager.InsertSketch(true)
Part.ShowNamedView2('Isometric', 7)

% Extrude Circle
Part.FeatureManager.FeatureExtrusion2(true, false, false, 0, 0,
s_thick, s_thick, false, false, false, false, 0, 0, false, false,
false, false, true, true, true, 0, 0, false);

% Base blade profile
Part.Extension.SelectByID2('Front Plane', 'PLANE', 0, 0, 0, false, 0,
[], 0);
Part.InsertCurveFileBegin
for jj = 1:length(XX)
    Part.InsertCurveFilePoint(XX(jj),YY(jj),0);
end
Part.InsertCurveFileEnd;
Part.ClearSelection2(true)

%Converts Curve to Sketch
Part.Extension.SelectByID2('Front Plane', 'PLANE', 0, 0, 0, false, 0,
[], 0);
Part.SketchManager.InsertSketch(true)
Part.Extension.SelectByID2('Curve1', 'REFERENCECURVES', 0, 0, 0, true,
0, [], 0);
Part.SketchManager.SketchUseEdge2(false);


%Scale Blade
Part.SketchManager.CreateCenterLine(0, 0, 0, 1, 0, 0)
Part.SetPickMode
Part.Extension.SelectByID2('Spline2', 'SKETCHSEGMENT', 0, 0, 0, true,
0, [], 0);
Part.Extension.SelectByID2('Line1', 'SKETCHSEGMENT', 0, 0, 0, true, 0,
[], 0);
Part.Extension.ScaleOrCopy(false, 1, 0, 0, 0, 1);

%Delete Curve
Part.SketchManager.InsertSketch(true);
Part.Extension.SelectByID2('Curve1', 'REFERENCECURVES', 0, 0, 0, false,
0, [], 0);
Part.EditDelete;

%Move Profile
Part.Extension.SelectByID2('Sketch2', 'SKETCH', 0, 0, 0, false, 0, [],
0);
Part.EditSketch
Part.Extension.SelectByID2('Spline2', 'SKETCHSEGMENT', 0, 0, 0, true,
0, [], 0);
Part.Extension.SelectByID2('Line1', 'SKETCHSEGMENT', 0, 0, 0, true, 0,
[], 0);
```

```
Part.Extension.MoveOrCopy(false, 1, true, 0, 0, 0, 0, ((radius)-
((2.5)*thickness*cord)), 0); %coefficient = 1.9 for .15 &.2
Coefficient = 1 for 0.1

%Extrude Cut
Part.FeatureManager.FeatureCut3(true, false, true, 1, 0, s_thick,
s_thick, false, false, false, false, 0, 0, false, false, false, false,
false, true, true, true, true, false, 0, 0, false);

%Add Axis & Pattern
Part.Extension.SelectByID2('Point1@Origin', 'EXTSKETCHPOINT', 0, 0, 0,
true, 0, [], 0);
Part.Extension.SelectByID2('', 'FACE', 0, 0, 0, true, 0, [], 0);
Part.InsertAxis2(true);
Part.Extension.SelectByID2('Cut-Extrude1', 'BODYFEATURE', 0, 0, 0,
true, 0, [], 0);
Part.ActivateSelectedFeature;
Part.Extension.SelectByID2('Cut-Extrude1', 'BODYFEATURE', 0, 0, 0,
false, 4, [], 0);
Part.Extension.SelectByID2('Axis1', 'AXIS', 0, 0, 0, true, 1, [], 0);
Part.FeatureManager.FeatureCircularPattern3(n_blades, 2*pi, false,
'NULL', false, true);

% Rotor is saved and documents closed
Part.SaveAs3([pwd '\NACA0018r7neg2.X_T'], 0, 0);
Part.SaveAs3([pwd '\NACA0018r7neg2.SLDPRT'], 0, 2);

% Revert to user interface and zoom to fit
Part.SketchManager.AddToDB = false;
Part.SketchManager.DisplayWhenAdded = true;
```

THIS PAGE INTENTIONALLY LEFT BLANK

APPENDIX F. MATLAB CODE FOR MONITORING TURBINE 1 AND 2, AND SUNNY ISLAND STATUS

```
% This is a program that obtains data from Sunny WebBox for Sunny
Islands and Wind Turbine 1 & 2.
%
clear all;close all;clc;

% Ask for number of inputs
Looptot = input('How many data points would you like? ')
if isempty(Looptot)
    Looptot = '5';
end



i = 1;
fprintf('Information from Sunny WebBox for Turbine 2\n')
fprintf(' Pwr Freq| Pwr 2 Grid| Turbine Current| Run \n');
fprintf('    Hz   |     W     |     Amps       |  #  \n');

% Initiating writing data for wind turbine 1:
% Webdatt1 = fopen('swbturb1_15SEP14.txt', 'w');
% fprintf(Webdatt1,'Information from Sunny WebBox for Turbine 1\n');
% fprintf(Webdatt1,' Pwr Freq| Pwr 2 Grid| | Turbine Current| Run \n');
% fprintf(Webdatt1,'   Hz    |      W      |     Amps       |  #  \n');

% Initiating writing data for wind turbine 2:
Webdatt2 = fopen('swbturb2_27OCT14.txt', 'w');
fprintf(Webdatt2,'Information from Sunny WebBox for Turbine 2\n');
fprintf(Webdatt2,' Pwr Freq| Pwr 2 Grid| | Turbine Current| Time \n');
fprintf(Webdatt2,'   Hz    |      W      |     Amps       | Date#
\n');

% Initiating writing data for Sunny Island Microgrid:
WebdatSI = fopen('swbSI1_27OCT14.txt', 'w');
fprintf(WebdatSI,'Information from Sunny WebBox from the Sunny
Island\n');
fprintf(WebdatSI,' Energy Absorb| Energy Fed| Batt SOC| Ext Volt| Run
\n');
fprintf(WebdatSI,'      kWh     |    kWh    | percent  |   Volts | #
\n');
tstart = tic;

% Assigning website for inputs
%urlt1=
'http://192.168.0.168/plant_devices_devfrm.htm?DevKey=WR5KU010:20021061
78&DevClass=Sunny%20Mini%20Central&group=PARENT';
urlt2 =
'http://192.168.0.168/plant_current.htm?DevKey=WR5KU010:2002106136&DevC
lass=Sunny%20Mini%20Central';
```

```
urlsi =
'http://192.168.0.168/plant_current.htm?DevKey=SI6048UH:1260019920&DevC
lass=Sunny%20Island';

% Preallocating the variables to improve efficiency of the program
% Pfq1 = zeros(1, Looptot);
% PtG1 = zeros(1, Looptot);
PtG = zeros(1, Looptot);
% TC1 = zeros(1, Looptot);
Pfq = zeros(1, Looptot);
PTG = zeros(1, Looptot);
TC = zeros(1, Looptot);
EgyCntIn =  zeros(1, Looptot);
EgyCntOut =  zeros(1, Looptot);
ExtVtg =  zeros(1, Looptot);
BatSOC =  zeros(1, Looptot);
t = zeros(1, Looptot);
%dts = zeros(4, Looptot);
while i <= Looptot

    % For the wind turbines 1 & 2, the AC power frequency (Hz), power
to
    % grid (W), and turbine current (Amps) are recorded using this
code.
    % For the Sunny Island microgrid, the Energy Absorbed (kWh), Energy
Fed
    % (kWh), Batter State of Charge (%), and External Voltage (V) are
    % recorded.

% Reading data for Turbine 1 (This portion is commented out due to
Turbine
% is not yet programmed.)
%     Pfq1(i) = urlfilter(urlt1, 'Fac');
%     PtG1(i) = urlfilter(urlt1, 'Pac');
%     TC1(i) = urlfilter(urlt1,'I-dif');
%     fprintf(Webdatt1,'   %3.2f  |   %3.2f     |    %4.2f       |
%1.0f   \n',...
%     Pfq1(i),PtG1(i),TC1(i),i);

% Reading Data for Turbine 2

    Pfq(i) = urlfilter(urlt2, 'Fac'); % Reading the AC frequency [Hz]
    PtG(i) = urlfilter(urlt2, 'Pac'); % Reading the AC power [W]
    TC(i) = urlfilter(urlt2,'I-dif'); % Reading the turbine current
[Amps]
    % Checking if the values after the variable are blank, then
assigning a
    % value of zero. The values of 8, 18, and 13 are the next line
number
    % after the AC frequency, AC power, and the turbine current
readings,
    % respectively. For example, if the value is blank after the 'Fac'
    % variable (line 7), then it would read a value of 8.
    if Pfq(i) == 8
```

```
        Pfq(i) = 0;
    end
    if PtG(i) == 18
        PtG(i) = 0;
    end
    if TC(i) == 13
        TC(i) = 0;
    end
    % Outputing the values to a tabular format for display
    fprintf('   %3.2f   |   %3.2f   |    %4.2f       |  %1.0f   \n',...
        Pfq(i),PtG(i),TC(i),i);


% Reading data for Sunny Island
    EgyCntIn(i) = urlfilter(urlsi, 'EgyCntIn');
    EgyCntOut(i) = urlfilter(urlsi, 'EgyCntOut');
    ExtVtg(i) = urlfilter(urlsi,'ExtVtg');
    BatSOC(i) = urlfilter(urlsi,'BatSoc');
    % fprintf('    %3.2f   |    %3.2f   |  %3.2f  |  %3.2f | %1.0f
\n',...
    %    EgyCntIn(i),EgyCntOut(i),ExtFrq(i),ExtVtg(i),i);
    % Recording to observed results to a text file for later analysis
    fprintf(WebdatSI,'    %3.2f   |    %3.2f   |  %3.2f  |  %3.2f |
%1.0f   \n',...
        EgyCntIn(i),EgyCntOut(i),BatSOC(i),ExtVtg(i),i);
    t(i) = now;
    %dts(i) = datestr(t(i));
    fprintf(Webdatt2,'   %3.2f  |   %3.2f     |    %4.2f       |  %1.0f
\n',...
        Pfq(i),PtG(i),TC(i),t(i));
    i = i + 1;
    pause(1);
end
% Determining the elapsed time to run the loop
telapsed1 = toc(tstart)
% fprintf(Webdatt1, '\n Total Elapsed time: %4.4g secs\n', telapsed1);
% fclose(Webdatt1);
fprintf(Webdatt2, '\n Total Elapsed time: %4.4g secs\n', telapsed1);
% ct = cellstr(datestr(t));
% fprintf(Webdatt2,'the date time is: %4.4g\n',ct)
fclose(Webdatt2);
fprintf(WebdatSI, '\n Total Elapsed time: %4.4g secs\n', telapsed1);
fclose(WebdatSI);
fprintf(' Total Elapsed time: %4.4g secs for %4.0f data points\n',...
    telapsed1, Looptot)
% Outputting the collected data from the text format to screen
%type swbturb1_15SEP14.txt
type swbturb2_27OCT14.txt
type swbSI1_27OCT14.txt

% Plotting out the desired information with the independent variable
being
% time in the format of (HH:mm)

% Turbine 1 Plot
```

```
% subplot(3,1,1)
% plot(t,Pfq1)
% datetick('x',21)
% ylabel('Pwr Freq (Hz)')
% subplot(3,1,2)
% plot(t,PtG1)
% datetick('x',21)
% ylabel('Pwr 2 Grid(W)')
% subplot(3,1,3)
% plot(t,TC1)
% datetick('x',21)
% ylabel('Turbine Current (Amp)')
% xlabel('Time (hh:mm:sec)')

% Turbine 2 Plots
% The plots consist of 1) AC frequency vs. time; 2) AC Power vs. time;
and
% 3) Turbine Current vs. time.
figure
subplot(3,1,1)
plot(t,Pfq)
datetick('x',21)
ylabel('Pwr Freq (Hz)')
subplot(3,1,2)
plot(t,PtG)
datetick('x',21)
ylabel('Pwr 2 Grid(W)')
subplot(3,1,3)
plot(t,TC)
datetick('x',21)
ylabel('Turbine Current (Amp)')
xlabel('Time (hh:mm:sec)')

% Sunny Island Plots
% The plots consist of 1) External Voltage vs. Time; 2) Energy Fed to
the
% micro-grid vs. time; and 3) Battery State of Charge vs. time
figure
subplot(3,1,1)
plot(t,ExtVtg)
datetick('x',21)
ylabel('ExtVtg (Volts)')
subplot(3,1,2)
plot(t,EgyCntOut)
datetick('x',21)
ylabel('Energy Fed(kWh)')
subplot(3,1,3)
plot(t, BatSOC)
datetick('x',21)
ylabel('Battery State of Charge (%)')
xlabel('Time (hh:mm:sec)')
```

LIST OF REFERENCES

[1] Environmental and Energy Study Institute. (2011, July).*DOD's energy efficiency and renewable energy initiatives.* Environmental and Energy Study Institute. Washington, DC. [Online]. Available: http://www.eesi.org/files/dod_eere_factsheet_072711.pdf.

[2] Office of the Deputy Under Secretary of Defense (Installation and Environment). (2014, June). *Energy management reports*. U.S. Dept. of Defense. Washington, DC. [Online]. Available: http://www.acq.osd.mil/ie/energy/energymgmt_report/main.shtml.

[3] W. M. Solis. "Defense management: DOD needs to increase attention on fuel demand management at forward-deployed location," U.S. Government Accountability Office, Washington, DC, GAO-09-300, Feb. 2009

[4] M. Picow. (2010, July 19). Record high summer temperatures are also scorching the Middle East. [Online]. Available: http://www.greenprophet.com/2010/07/climate-change-middle-east/.

[5] 1 Gigawatt Task Force.(2012, Oct.) Department of the Navy strategy for renewable energy. U.S. Dept. of the Navy, Washington, DC. [Online]. Available: http://www.secnav.navy.mil/eie/ASN%20EIE%20Policy/DASN_EnergyStratPlan_Finalv3.pdf.

[6] Glossary of energy-related terms. (2013, 20 Aug.). U.S. Dept. of Energy, 20 August 2013. [Online]. Available: http://energy.gov/eere/energybasics/articles/glossary-energy-related-terms#R.

[7] T. F. Stocker et al., "IPCC,2013: Climate Change 2013 The Physical Science Basis," Intergovernmental Panel on Climate Change, Cambridge University Press, New York, 2013.

[8] A. Togelou et al., "Wind power forecasting in the absence of historical data," *IEEE trans. on sustainable energy*, vol. 3, no. 3, pp. 416–421, 2012.

[9] Solar thermal energy. (2008). [Online]. Available: http://www.solar-thermal.com/solar_vs_pv.html

[10] A. J. Cavallo, "Energy storage technologies for utility scale intermittent renewable energy systems," *J. of Solar Energy Engineering*, vol. 123, pp. 387–389, Nov. 2001.

[11] D&R International, Ltd. (2012, Mar.) 2011 Building Energy Data Book. [Online]. Available: http://buildingsdatabook.eren.doe.gov/DataBooks.aspx

[12] T. Hinke, "Hot thermal storage," M.S. thesis, Dept. Mech. and Aerosp. Eng., Naval Postgraduate School, Monterey, CA, 2014.

[13] C. Borgnakke and R. E. Sonntag, *Fundamentals of Thermodynamics*, 7th ed., Hoboken: John Wiley & Sons, Inc., 2009. pp. 759.

[14] L. M. Olsen, "Initial investigation of a novel thermal storage concept as part of a renewable energy system," M.S. thesis, Dept. Mech. and Aerosp. Eng., Naval Postgraduate School, Monterey, CA, 2013.

[15] P. O. Kriett and M. Salani, "Optimal control of a residential microgrid," *Energy*, vol. 42, no. 1, pp. 321–330, 2012.

[16] N. Hatziargyriou, H. Asano et al., "Microgrids: An Overview of Ongoing Research, Development, and Demonstration Projects," *IEEE Power & Energy Mag.*, vol. 5, no. 4, pp. 78–94, 2007.

[17] S. Marcacci. (2013, Apr. 3). Over 400 Microgrid Projects Underway En Route to $40 Billion Market. [Online]. Available: http://cleantechnica.com/2013/04/03/over-400-microgrid-projects-underway-en-route-to-40-billion-market/

[18] A. Chan. (2013 Winter). Nation's Largest Microgird Online. Winter 2012. [Online]. Available: http://www.rmi.org/nations_largest_microgrid_online_esj_article

[19] B. H. Newell, "The evaluation of HOMER as a Marine Corps expeditionary energy pre-deployment tool," M.S. thesis, Dept. Elect. and Comput. Eng., Naval Postgraduate School, Monterey, CA, 2010.

[20] P. Schubel and R. Crossley, "Wind Turbine Blade Design," *Energies*, vol. 5, pp. 3425–3449, 2012.

[21] UGE Visionare 5. (2014). Urban Green Energy Inc. [Online]. Available: http://www.urbangreenenergy.com/products/visionair5

[22] H. C. Davis, Wind-electric ice making for developing world villages, Boulder: M.S. Thesis, Dept. Civil Eng., Environmental and Architectural Eng., Univ. Colorado, Boulder, CO, 1994.

[23] K. C. Taylor, "Method for VAWT placement on a complex building structure," M.S. thesis, Dept. Mech. and Aerosp. Eng., Naval Postgraduate School, Monterey, CA 2013.

[24] J. Pascual et al., "Implementation and control of a residential microgrid based on renewable energy sources, hybrid storage systems and thermal controllable loads," presented at *Energy Conversion Congress and Exposition (ECCE)*, Denver, CO, 2013. doi: 10.1109

[25] M. Robinson and M. Scepaniak. (2007, Oct. 1). Applying VFDs to refrigeration systems. [Online]. Available: http://hpac.com/motors-drives/applying_vfds_refrigeration

[26] Modbus FAQ. (2014). Modbus Organization, Inc. [Online]. Available: http://www.modbus.org/faq.php

[27] Energy systems technology evaluation program (ESTEP). (2013, June 17). U.S. Navy. [Online]. Available: http://www.nps.edu/Academics/OtherPrograms/Energy/Research/s-t_ESTEP.html

[28] D. Smalley. (2012, Oct. 18). Energize: ONR supports new energy partnership. U.S. Navy. [Online]. Available: http://www.onr.navy.mil/Media-Center/Press-Releases/2012/Energy-Systems-Technology-ESTEP-ONR.aspx

[29] P. Ferrini. (2009). AURORA wind box interface installation and operator's manual. Power-One. Camarillo. pp. 6–8.

[30] G. V. Hobson, private communication. MATLAB code. Naval Postgraduate School, Monterey, CA, June 2014.

[31] SST k-omega model. (2011, Feb. 28). CFD-online.com. [Online]. Available: http://www.cfd-online.com/Wiki/SST_k-omega_model.

[32] C. Abbey and G. Joos, "Supercapacitor energy storage for wind energy applications," *IEEE Trans. Ind. Appl.* vol. 43, no. 3, pp. 769–776, May/June 2007. [Online]. Available: http://ieeexplore.ieee.org/stamp/stamp.jsp?tp=&arnumber=4214991

THIS PAGE INTENTIONALLY LEFT BLANK

INITIAL DISTRIBUTION LIST

1. Defense Technical Information Center
   Ft. Belvoir, Virginia

2. Dudley Knox Library
   Naval Postgraduate School
   Monterey, California